

MERDAN ALTYBAYEV

B. ENG. (HONS) PETROLEUM ENGINEERING

JANUARY 2015

OXIDATION AND HOT CORROSION BEHAVIOR OF  
 $\text{Cr}_3\text{C}_2$  25 (Ni20Cr) THERMAL SPRAY COATING

**MERDAN ALTYBAYEV**

PETROLEUM ENGINEERING  
UNIVERSITI TEKNOLOGI PETRONAS  
JANUARY 2015



**Oxidation and Hot Corrosion Behaviour of Cr<sub>3</sub>C<sub>2</sub> 25 (Ni20Cr)  
Thermal Spray Coating**

by

MERDAN ALTYBAYEV

14644

Dissertation submitted in partial  
fulfilment of the requirements for the  
Bachelor of Engineering (Hons)  
(Petroleum)

JANUARY 2015

Universiti Teknologi PETRONAS  
Bandar Seri Iskandar  
31750 Tronoh  
Perak Darul Ridzuan

# **CERTIFICATION OF APPROVAL**

## **Oxidation and Hot Corrosion Behaviour of Cr<sub>3</sub>C<sub>2</sub> 25 (Ni20Cr) Thermal Spray Coating**

by

MERDAN ALTYBAYEV

14644

A project dissertation submitted to the  
Petroleum Engineering Programme  
Universiti Teknologi PETRONAS  
in partial fulfilment of the requirement for the  
BACHELOR OF ENGINEERING (Hons)  
(PETROLEUM)

Approved by,

---

(Assoc. Prof. Dr. Subhash Kamal)

UNIVERSITI TEKNOLOGI PETRONAS

TRONOH, PERAK

January 2015

## **CERTIFICATION OF ORIGINALITY**

This is to certify that I am responsible for the work submitted in this project, that the original work is my own except as specified in the references and acknowledgements, and that the original work contained herein have not been undertaken or done by unspecified sources or persons.

---

MERDAN ALTYBAYEV

## **ABSTRACT**

High temperature oxidation and corrosion represents the most maleficent forms of surface degradation, which leads to the loss of mechanical strength and disastrous failure of structural and engineering components. They are generally encountered in materials used in turbines and aero engines, which operate in high temperature and corrosive environments. Due to extensive employment of these materials, the high temperature oxidation and corrosion behaviour has been the subject of intense investigation for the past several years. Therefore, the present study investigates the oxidation and hot corrosion behaviour of Cr<sub>3</sub>C<sub>2</sub> 25 (Ni20Cr) thermal spray coating on Austenitic stainless steels (AISI 304) exposed to extreme corrosive (Na<sub>2</sub>SO<sub>4</sub>) environment, at 900 °C. HVOF (High Velocity Oxy-Fuel) method will be used to apply coating on the surface of substrate material. The weight change measurements made on the substrate during the experiments will be used to determine the kinetics of oxidation and hot corrosion. Surface structure and morphology will be evaluated using X-ray diffraction (XRD), X-ray mapping and field emission scanning electron microscope (FESEM).

## **ACKNOWLEDGEMENTS**

First of all, I would like to extend special appreciation to my supervisor, Assoc. Prof. Dr. Subhash Kamal, for aiding me supportively, who through his professional experience and expertise, have guided me with great knowledge, insights and enthusiasm to ensure development of ideas and progressive learnings. His invaluable help of constructive comments and suggestions throughout the experimental and thesis works have contributed to the success of this research.

Furthermore, I would like to thank my internal examiner, Dr. Shiferaw Regassa Jufar for giving me constructive feedbacks and areas to improve upon.

I would like to take it to express my utmost and sincere gratitude to the people who have provided such a great deal of aid and assistance in undergoing the research project together. Also I would like to extend my appreciation to Mr. Muhammad Danial and Mr. Mohd Kamarul, technologists from Mechanical Engineering department for guiding me through the procedures of the experiments. Not to forget, I would also like to thank Mr. David Chue from Metatech Sdn. Bhd. for his helps in providing the HVOF coating services.

Last but not least, I would like to thank Universiti Teknologi PETRONAS (UTP) for providing necessary facilities that aided in developing progress for this Final Year Project.

## TABLE OF CONTENT

<b>CERTIFICATE OF APPROVAL</b> .....	i
<b>CERTIFICATE OF ORIGINALITY</b> .....	ii
<b>ABSTRACT</b> .....	iii
<b>ACKNOWLEDGEMENT</b> .....	iv
<b>CHAPTER 1: INTRODUCTION</b> .....	1
1.1 Background .....	1
1.2 Problem Statement .....	2
1.3 Objectives .....	3
1.4 Scope of Study.....	3
<b>CHAPTER 2: LITERATURE REVIEW</b> .....	4
<b>CHAPTER 3: METHODOLOGY</b> .....	7
3.1 Coating Powder .....	7
3.2 Sample Preparation .....	8
3.3 Experimental Procedure .....	9
3.3.1 Hot Corrosion Test .....	9
3.3.2 Oxidation Test .....	10
3.4 Process Flow .....	11
3.5 Process Flow Chart .....	12
3.6 Gantt Chart and Milestones.....	13
<b>CHAPTER 4: RESULTS AND DISCUSSION</b> .....	15
4.1 Thermogravimetric analysis .....	15
4.2 X-ray Diffraction analysis .....	18
4.3 FE-SEM/EDAX analysis.....	22
4.3.1 Surface morphology of the scales .....	22
4.3.2 X-ray mapping.....	25
4.5 Discussion .....	28
<b>CHAPTER 5: CONCLUSION AND RECOMMENDATION</b> .....	30
5.1 Conclusion.....	30
5.2 Recommendation.....	31
<b>REFERENCES</b> .....	32
<b>APPENDICES</b> .....	34

## LIST OF FIGURES

Figure 1: Oxidation and hot corrosion of the AISI 304 .....	2
Figure 2: Thermal spray coating process .....	4
Figure 3: HVOF process .....	5
Figure 4: Sample preparation steps .....	8
Figure 5: Oxidation and hot corrosion tested specimens .....	10
Figure 6: The sequence of work.....	11
Figure 7: Process Flow Chart for FYP .....	12
Figure 8a: Weight change vs time plot for oxidation.....	16
Figure 8b: Weight change vs time plot for hot corrosion .....	16
Figure 9a: Cumulative weight change vs time plot for oxidation.....	17
Figure 9b: Cumulative weight change vs time plot for hot corrosion.....	17
Figure 10: X-ray diffraction patterns of bare AISI 304 (oxidation).....	18
Figure 11: X-ray diffraction patterns of coated AISI 304 (oxidation).....	19
Figure 12: X-ray diffraction patterns of bare AISI 304 (hot corrosion) .....	20
Figure 13: X-ray diffraction patterns of coated AISI 304 (hot corrosion).....	21
Figure 14: FE-SEM/EDAX analysis for bare AISI 304 (oxidation).....	22
Figure 15: FE-SEM/EDAX analysis for bare AISI 304 (hot corrosion).....	23
Figure 16: FE-SEM/EDAX analysis for coated AISI 304 (oxidation) .....	24
Figure 17: FE-SEM/EDAX analysis for coated AISI 304 (hot corrosion) .....	24
Figure 18: X-ray mapping of bare AISI 304 (oxidation).....	25
Figure 19: X-ray mapping of coated AISI 304 (oxidation).....	26
Figure 20: X-ray mapping of bare AISI 304 (hot corrosion).....	27
Figure 21: X-ray mapping of coated AISI 304 (hot corrosion) .....	27

## LIST OF TABLES

Table 1: Chemical composition of AISI 304 stainless steel .....	8
Table 2: Sample preparation parameters.....	8
Table 3: HVOF process parameters .....	9
Table 4: Gantt chart for FYP II.....	13
Table 5: Key Milestones .....	14

## ABBREVIATIONS AND NOMENCLATURES

<b>AISI 304</b>	Austenitic Stainless Steel grade
<b>C</b>	Carbon
<b>Cr</b>	Chromium
<b>Ni</b>	Nickel
<b>Fe</b>	Iron
<b>Na<sub>2</sub>SO<sub>4</sub></b>	Sodium Sulfate
<b>NiCr<sub>2</sub>O<sub>4</sub></b>	Nickel Chromium Oxide
<b>Cr<sub>3</sub>C<sub>2</sub></b>	Chromium Carbide
<b>Cr<sub>2</sub>O<sub>3</sub></b>	Chromium Oxide
<b>NiO</b>	Nickel Oxide
<b>Fe<sub>2</sub>O<sub>3</sub></b>	Iron (III) Oxide
<b>HVOF</b>	High velocity oxy-fuel
<b>MSDS</b>	Material Safety Data Sheet
<b>FE-SEM</b>	Field Emission Scanning Electron Microscope
<b>XRD</b>	X-Ray diffraction

# CHAPTER 1

## INTRODUCTION

### 1.1 Background

Choosing a theme of problem-oriented research of this dissertation is due to the needs of the engineering, shipbuilding and, above all, the aviation industry in the development and use of new classes of lightweight materials capable of operating at extreme operation conditions.

When metals are exposed to air at high-temperature environments, some parts or entire metal converted into oxides is called oxidation. Oxidation is highly dangerous type of degradation that metal can encounter. Once the oxidation process have started it's inevitable, but sometimes, after certain period oxidation reduces, because of the protective layer formed on the surface of metals. In most cases oxidation continues resulting in progressive metal damage, eventually ending with component failure.

Substandard combustible fluids utilised in the industry to generate energy, often contain complex mixture of molten salts ( $\text{Na}_2\text{SO}_4 + \text{V}_2\text{O}_5$ ). These salts form compounds with the melting point (up to 600 °C). During high temperature operations (>600 °C) minerals start heavily settle on exposed metals, inevitably causing disastrous corrosion phenomena.

Resistance to oxidation and corrosion is a requisite for superalloys whether used in high temperature conditions or not. However, corrosion failures of these superalloys have been observed, due to extended period of exposure to such harsh environments.

Thermal spray coatings can serve as the best technique yet developed to evade the corrosive fluids from contacting the substrate metal surface, by means of the protective layer created. There are several types of coatings techniques and coating powders available in the market.

## 1.2 Problem Statement

Austenitic stainless steel (AISI 304) offers high oxidation/corrosion resistance properties, also has excellent form and weld abilities. Such features allow the AISI 304 to be used in varieties of applications in both food and energy industries. Nevertheless, it's not sufficient corrosion resistant in corrosive, sodium sulfate ( $\text{Na}_2\text{SO}_4$ ) and vanadium pentoxide ( $\text{V}_2\text{O}_5$ ) solutions.



*Figure 1: Oxidation and hot corrosion of the AISI 304(Hermanek, 2014)*

Bare metal components exposed to these conditions and upon damage, need to be replaced which may prove to be costly, due to replacement and even changes in the dimension or the properties of the components.

One effective way to overcome this problem is to apply thermal spray coating on substrate material and study behaviour of both coated and uncoated materials in highly corrosive medium.

### **1.3 Objectives**

To complete this study a few objectives were outlined to guide the research process. These objectives are listed below:

- ❖ To analyse and study the oxidation and hot corrosion resistance properties of AISI 304 stainless steel.
- ❖ To analyse and study the oxidation and hot corrosion behaviour of substrate metal which have been coated using Cr<sub>3</sub>C<sub>2</sub> 25 (Ni20Cr) thermal spray coating, using HVOF (High Velocity Oxy-Fuel) technique.

### **1.4 Scope of Study**

The scope of this dissertation includes analysing the oxidation and hot corrosion behaviour of AISI 304 stainless steel metal and the effects of thermal spray coating on corrosion/oxidation resistance. The physic-chemical characteristics and morphologies of the metal substrates will be investigated by using X-Ray Diffraction (XRD), Field Emission Scanning Electron Microscopy (FESEM).

## CHAPTER 2

### LITERATURE REVIEW

Today, in all sectors of industry, the catch phrase ‘better, faster, cheaper’ is common and valid, production demanding requirements and aggressive service conditions often lead to the premature loss of components or system function failures. Development of technologies for the production of materials with special microstructure, reinforcing and modifying alloying and reliable protective coatings will resolve that ever-increasing industry demand in the future using them in the most extreme operating conditions. Thus, a lot of researches done to study and analyse the hot corrosion and oxidation behaviour of the materials used in extreme conditions of the growing industry demands by reinforcing the metals with thermal spray coatings. (Amardeep Singh Kang, 2012)

Thermal spray coating is a process of depositing smelted materials on the substrate at high velocity. Materials used in this process vary from powder to ceramic rods, wires or molten materials. Several techniques of coating processes utilized by industry are depending on the demand. (D. K. Goyal, 2011) **Figure 2** indicates how the spray material (in our case powder) is melted using electric or gas heating, after which is being accelerated and impacted on the surface of substrate, producing a coating as a result.

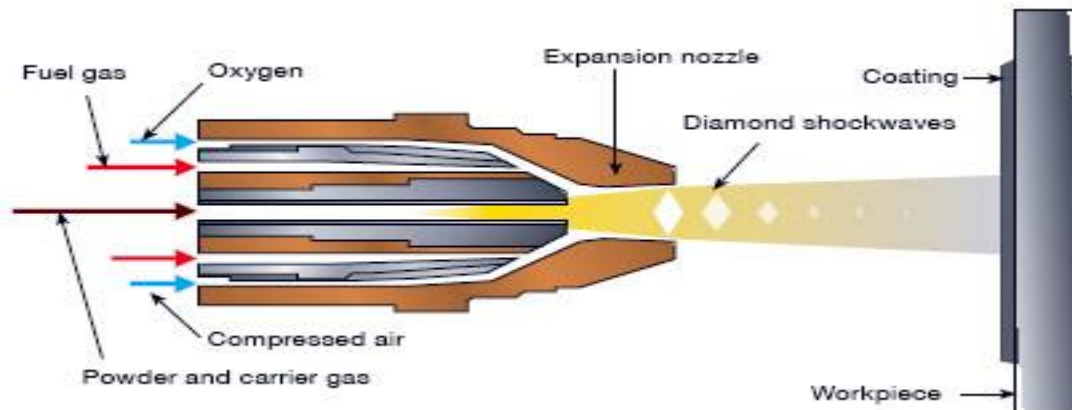


Figure 2: Thermal spray coating process (Hermanek, 2014)

According to Davis (2004), there are several types of thermal spray processes available in the industry, including:

1. Flame powder
2. Wire flame
3. High velocity oxy-fuel (HVOF)
4. Detonation gun (D-Gun)
5. Electric and plasma arc processes

HVOF process uses a combination of inflammable gases including propane, hydrogen and sometimes kerosene. The HVOF gun differs from other guns producing higher velocities and higher burning temperature. Inside the combustion chamber, the coating powder is expanded and expelled outward through the nozzle at very high velocity as indicated in **Figure 3**. The HVOF process will be used due to its high deposition efficiency, compared to the other thermal spray techniques, combined with much lower cost than laser technique. (Cho, 2009)



*Figure 3: HVOF process (Hermanek, 2014)*

Y.F. Yan (2013), analysed the hot corrosion behaviour of Austenitic stainless steel in  $\text{Na}_2\text{SO}_4$  at  $635^\circ\text{C}$  and compared it various alloys and commercial steel. They have discovered that the tested material showed an excellent resistance to corrosion, despite a fact that initially aluminium oxide ( $\text{Al}_2\text{O}_3$ ) layer was formed, followed by chromium oxide ( $\text{Cr}_2\text{O}_3$ ) formation on the surface of the metal, it efficiently subdued further deterioration.

N. Padhy (2010), evaluated the corrosion performance of TiO<sub>2</sub> coated austenitic stainless steel 304L in acidic medium. Whereas, Jianqiang Zhang (2013) have studied the improvement in oxidation/corrosion resistance of 304 SS in cyclic conditions after nano-crystalline coating was applied. Nano-crystalline 304 SS was compared with micro-crystalline 304 SS for oxidation behaviour in (10% H<sub>2</sub>O) air at 900 °C. It was found that the micro-crystalline alloy produced lesser resistance, resulting in substantial oxidation, but nano-crystalline 304 SS endured rapid oxidation, but then reaction slowed down.

R. J. Subhash Kamal, Satya Prakash (2009), on the other hand investigated behaviour of Cr<sub>3</sub>C<sub>2</sub>-NiCr cermet thermally sprayed coatings against hot corrosion on various superalloys. The experiments were carried out on both coated and raw superalloys in highly corrosive medium at high temperature (>900 °C) in cyclic conditions. Different types of analysing techniques were used to investigate the corrosion level. They have drawn the conclusion that cermet coated materials demonstrated better resistance to corrosion at high temperatures.

Thermal spray coatings offer cost-effective solutions for wide range of problems, such as hot corrosion, oxidation, wear of the components and erosion, depending on the coating method and the powders used. There are wide range of materials that can be used as substrates for coating such as alloys, oxide and non-oxide ceramics, carbides and etc. Therefore, a lot of studies have been and still being conducted using various substrate materials such as alloys and superalloys, using different types of spraying techniques, in order to achieve excellent hot corrosion and oxidation properties, enhancing the durability and serviceability.

## **CHAPTER 3**

### **METHODOLOGY**

In order to successfully complete this research, first author will have to:

- ❖ Number of agencies (some from China) providing coating powders, were contacted and requested the quotation of several coatings that we have chosen before, finally we selected Diamalloy 3004 powder form Metatech Sdn. Bhd.
- ❖ Number of local steel dealers, were contacted and requested the quotation on the Austenitic Stainless Steel (AISI 304), finally we acquired metal plate with dimension (400 mm x 400 mm x 5 mm) from TSA Industries Sdn. Bhd.

Once the necessary materials are obtained, there are few experiments planned to be done, as follows:

1. Substrates with/without coating in sodium sulfate ( $\text{Na}_2\text{SO}_4$ ) solution at 900 °C
2. Substrates with/without coating in chamber filled with air at 900 °C

#### **3.1 Coating powder**

This blended material mainly consist of chromium carbide ( $\text{Cr}_3\text{C}_2$ ) and nickel-chromium (NiCr) powders. The chromium carbide compound ensure serves as a hard phase that ensures wear resistance, while the nickel-chromium serves as an array that improves the hot corrosion resistance and overall coating integrity. Materials coated with these powder effectively deal with high temperature oxidation and hot corrosion. HVOF process attains much more uniform, well bonded and compact structure when used to apply coatings.(*N. Jegadeeswaran, 2014*)

### 3.2 Sample Preparation

In order to carry out the experiments to study and analyse the resistance behaviour to oxidation and hot corrosion of the thermal spray coatings, few samples of Austenitic Stainless Steel (AISI 304) have to be fabricated. The composition of substrate chosen for the present study is given in **Table 1**. (M. Mamatha Kumari, 2010)

*Table 1: Chemical composition of AISI 304 stainless steel*

Components	C	Cr	Ni	Fe	Mn	P	S	N	Si
Content (%)	0.08	18-20	8-12	Balance	2	0.045	0.03	0.10	0.75

Samples of dimension 30mm × 30 mm × 5 mm (thickness) will have to be cut from a plate and cleaned with sandpaper and then polished in polycrystalline diamond paste before an actual coating process. These samples then have to be coated using HVOF coating process. Desired sample preparation parameters are listed in the Table 2 (N. Padhy, 2010)

*Table 2: Sample preparation parameters*

Parameters	Details
Coating powder	Cr <sub>3</sub> C <sub>2</sub> -25NiCr (Sulzer Metco Diamalloy 3004)
Powder size	-45+5.5μm
Morphology	Blended
Substrate	AISI 304 Stainless Steel
Deposition technique	HVOF
Coating thickness	200 μm (±25 μm)

Sample preparation is done in the following steps as shown in **Figure 4**



*Figure 4: Sample preparation steps*

During sample preparations following setup parameters given in **Table 3**, were used in order to obtain the thickness range necessary for this particular study.

*Table 3: HVOF process parameters*

<b>Parameters</b>	<b>Details</b>
Fuel gas	CH <sub>4</sub>
Oxygen pressure (bar)	10.3
Fuel pressure (bar)	7.6
Air pressure (bar)	6.9
Oxygen flow rate, O <sub>2</sub> (NLPM)	279
Fuel flow rate, CH <sub>4</sub> (NLPM)	190
Air flow rate (NLPM)	361
Carrier gas flow rate, N <sub>2</sub> (NLPM)	12.5
Spray rate (g/min)	38 – 75
Spray distance (mm)	230
Deposit efficiency (%)	30

### **3.3 Experimental procedure**

#### **3.3.1 Hot corrosion test**

Cyclic studies will be performed for the prepared samples in highly corrosive medium (Na<sub>2</sub>SO<sub>4</sub>) and air. One cycle consist of 3 hour high temperature treatment and 25 minutes of room temperature cooling. The main reason behind implementing cyclic conditions is to simulate actual operation conditions. To measure the total corrosion rate, weight change measurements have to be taken with each cycle. Additionally samples go through some X-Ray based analyses for further oxidation/hot corrosion behaviour investigation.

First, we mix Na<sub>2</sub>SO<sub>4</sub> (25 wt %) in distilled water as our pre-selected corrosive salt environment. After we put samples to oven at about 250 °C for 30 min. to heat, which is essential for proper cohesion of the salt layer. Once sample is heated, a layer of Na<sub>2</sub>SO<sub>4</sub> solution was applied uniformly with camel hair brush. The content of salt deposited on each sample was approximately 3.0-4.0 mg/cm<sup>2</sup>.

After all the pre-experimental procedures were carried out, the specimens were placed in furnace at 900 °C to conduct hot corrosion test. At regular intervals (3 hrs) of 20 hrs, the samples were taken out and cooled at room temperature (25 °C) for 25 min., then weighted by an electronic balance to determine the weight change. This cyclic tests were executed on both coated and uncoated samples, to compare the hot corrosion resistance.

### 3.3.2 Oxidation test

The oxidation studies on Cr<sub>3</sub>C<sub>2</sub>-NiCr-coated and uncoated AISI 304 stainless steel samples were conducted at 3 hours intervals for 20 hours at 900 °C in regular furnace. After every 3 hours samples were cooled at room temperature (25 °C) for 25 min. This cyclic experiments the accelerated test conditions, which simulates the actual working conditions in real world. At the end of each cycle, weight change measurements were taken in order to formulate the kinetics of oxidation.

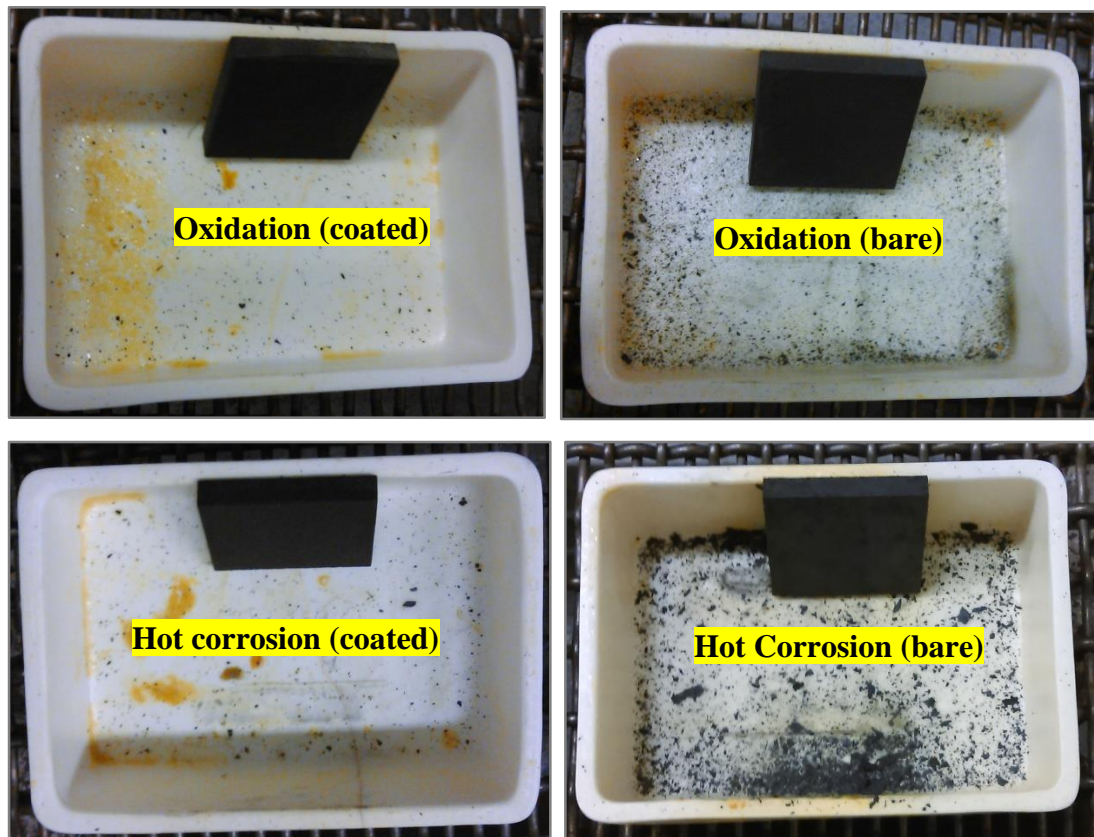


*Figure 5: Oxidation and hot corrosion tested specimens at 900 °C*

### 3.4 Process Flow

Figure below describes the sequence of work load expected to be performed in order to effectively complete the project in allocated time frame.

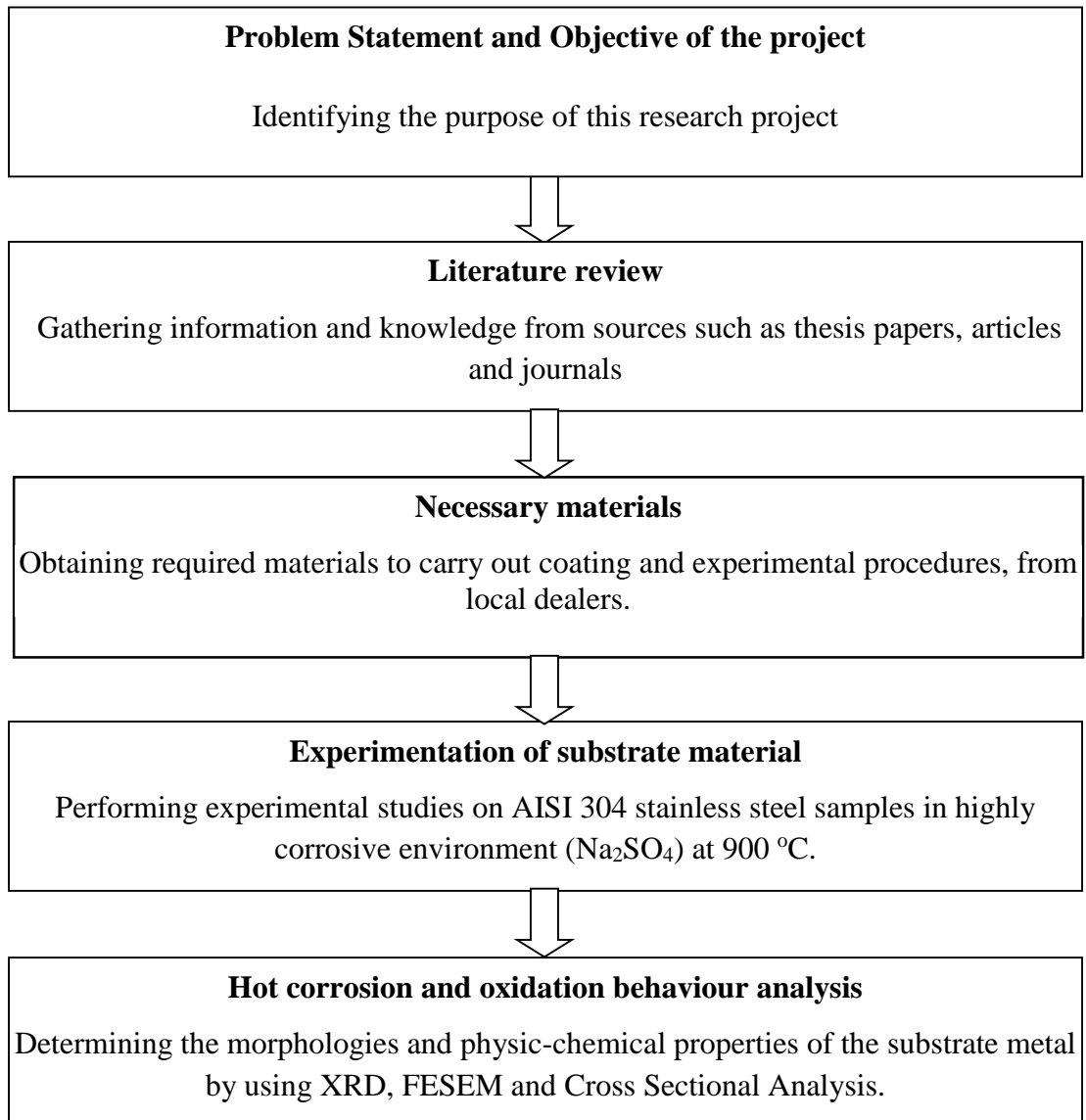


*Figure 6: The sequence of work*

### 3.5 Process Flow Chart

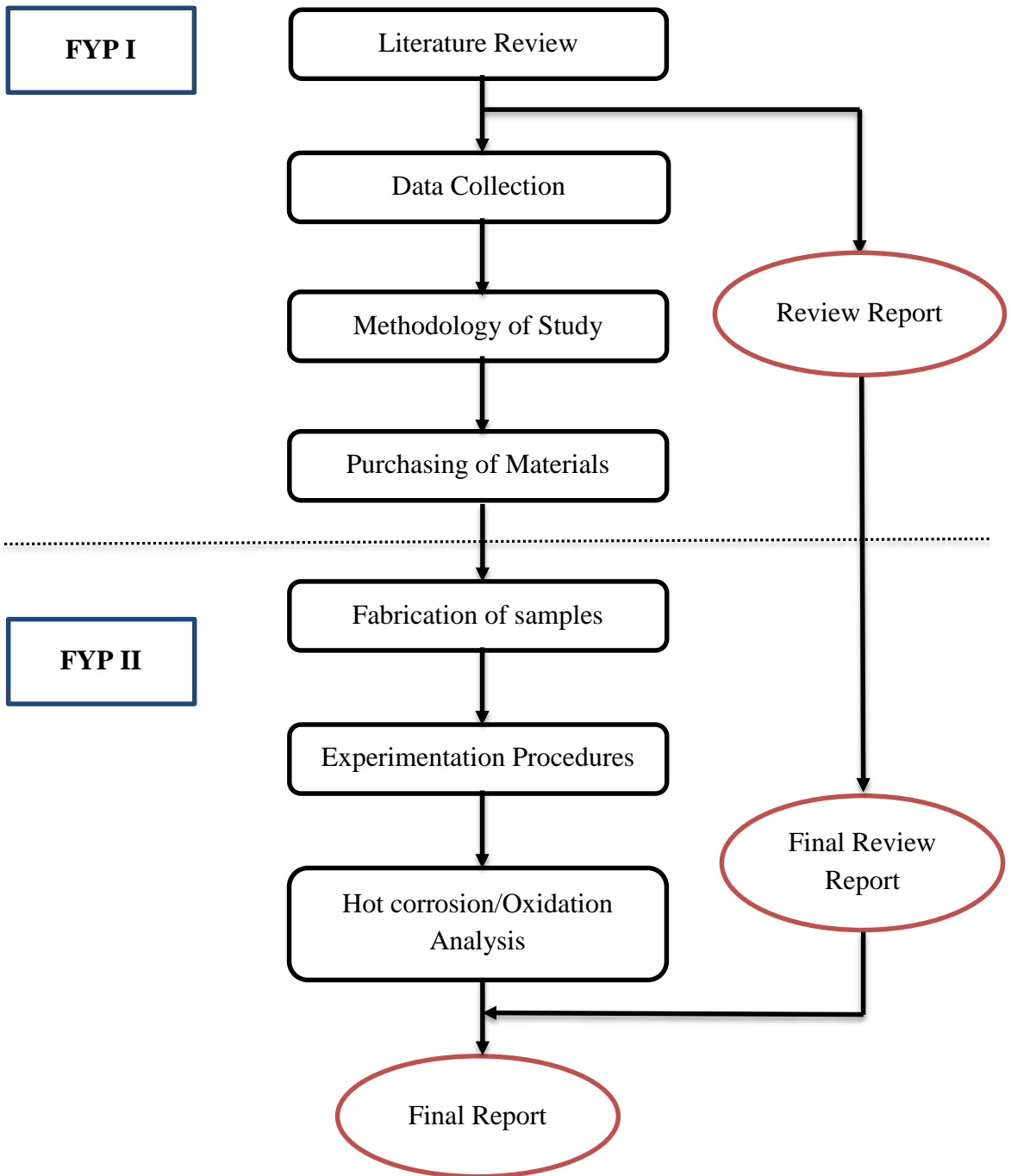


Figure 7: Process flow chart

### 3.6 Gantt Chart and Milestones

Table 4: Gantt Chart for FYP\_II

Week	1	2	3	4	5	6	7	8	9	10	11	12	13	14	15
Finalizing literature analysis	■	■	■												
Fabrication of samples (raw material)			●												
Finalizing order for coating powder				■	■										
Fabrication of samples (coated)						●									
Progress Report submission							●								
Monitoring the experimental procedures							■	■	■						
Results for experiments							■	■	■						
Pre-SEDEX presentation									●						
Analysis of the experimental results										■	■	■			
Draft Report submission												●			
Dissertation (Soft copy) submission												●			
Technical Paper submission												●			
Oral Presentation (Viva)														●	
Project Dissertation (Hard bound) submission															●

*Table 5: Key Milestones*

<b>Milestones</b>	<b>Dates (Year 2015)</b>
<b>Fabrication of samples (raw material)</b>	30 January
<b>Fabrication of samples (coating)</b>	24 February
<b>Progress Report submitted</b>	25 February
<b>Results for experimental procedures</b>	4 March
<b>Pre-SEDEX</b>	11 March
<b>Finalised results for experiments</b>	24 March
<b>Draft Report submission</b>	31 March
<b>Dissertation (Soft bound) submission</b>	31 March
<b>Technical Paper submission</b>	31 March
<b>Oral Presentation (Viva)</b>	13-14 April
<b>Project Dissertation (Hard Bound) submission</b>	29 April

## CHAPTER 4

### RESULTS AND DISCUSSION

#### 4.1 Thermogravimetric analysis

The hot corrosion kinetics were determined from the weight change vs time plots for samples, both bare and coated with  $\text{Cr}_3\text{C}_2\text{-NiCr}$  thermal spray coating, that undergo the hot corrosion test in extremely corrosive environment,  $\text{Na}_2\text{SO}_4$  solution at  $900\text{ }^\circ\text{C}$  for 20 hours as shown in the **Figures 8a and 8b**. It can be observed that all cases encountered an initial weight change.

During that period, the rate of formation of oxides on the free surface of samples is high. With the further exposure, the rate has slowed down, due to the growth of the oxide grains and reduction in diffusion pathway density. In the later cycles, corrosion samples started spalling/sputtering and falling outside of the experimental boat, so it became difficult to monitor actual weight change.

The weight change plot indicates that  $\text{Cr}_3\text{C}_2\text{-NiCr}$  coated specimens show a lower weight change compared to the bare specimens in corrosive molten salt medium at  $900\text{ }^\circ\text{C}$ , which is found to be more resistant to oxidation and hot corrosion.

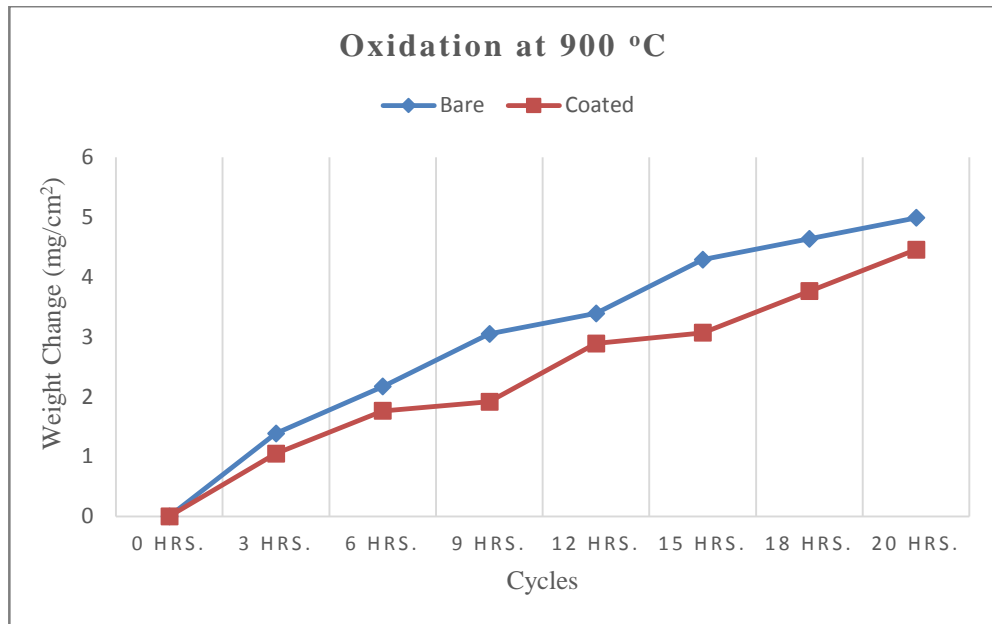


*Figure 8a: Weight change vs time plot for oxidation*

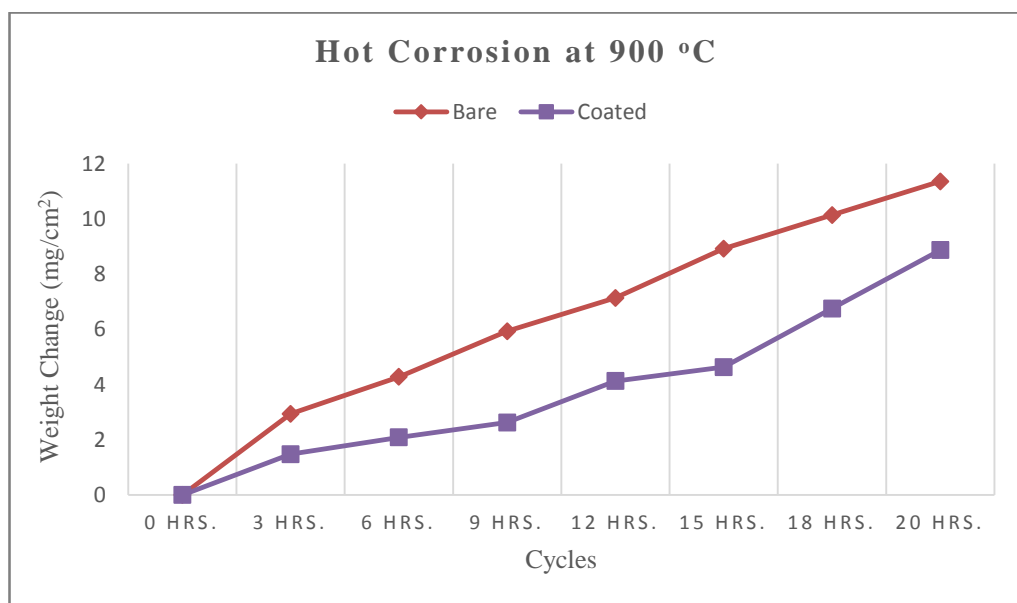


*Figure 8b: Weight change vs time plot for hot corrosion*

In general, the oxidation and hot corrosion behaviour of Cr<sub>3</sub>C<sub>2</sub>-NiCr coated AISI 304 stainless steel samples, follow nearly a parabolic rate law, as can be deduced from **Figure 8a and 8b**.

Cumulative weight change/area for bare and coated samples can be seen in **Figures 9a and 9b**.

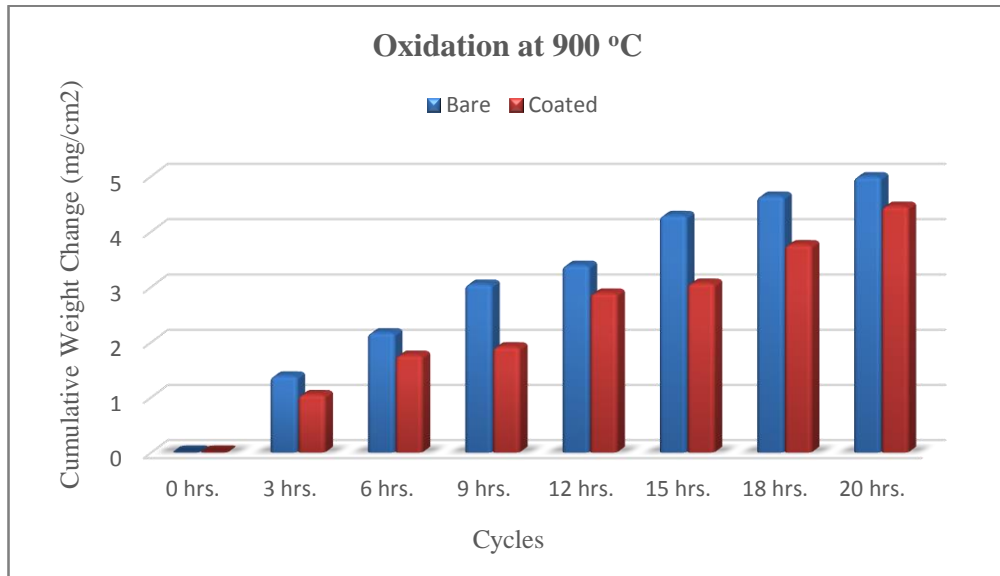


*Figure 9a: Cumulative weight change vs time plot for oxidation*

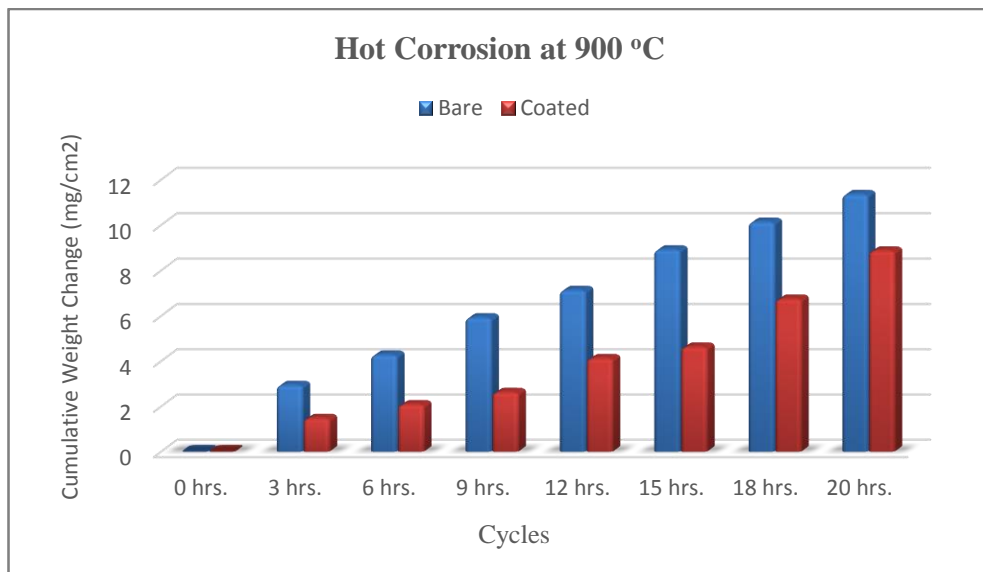


*Figure 9b: Cumulative weight change vs time plot for hot corrosion*

## 4.2 X-ray Diffraction (XRD) analysis

The X-ray diffraction (XRD) patterns for corroded surfaces of bare and  $\text{Cr}_3\text{C}_2$ -NiCr coated AISI 304 stainless steel samples subjected to  $\text{Na}_2\text{SO}_4$  molten salt environment and air at  $900\text{ }^\circ\text{C}$  for 20 hours are analysed in this section.

For bare austenitic stainless steel AISI 304 sample subjected to oxidation at  $900\text{ }^\circ\text{C}$ , the major phases detected were NiCr,  $\text{Cr}_3\text{C}_2$ ,  $\text{NiCr}_2\text{O}_4$ , whereas minor phases were  $\text{Cr}_2\text{O}_3$ , NiO, and  $\text{Fe}_2\text{O}_3$  as shown in X-ray diffraction patterns in the **Figure 10**.

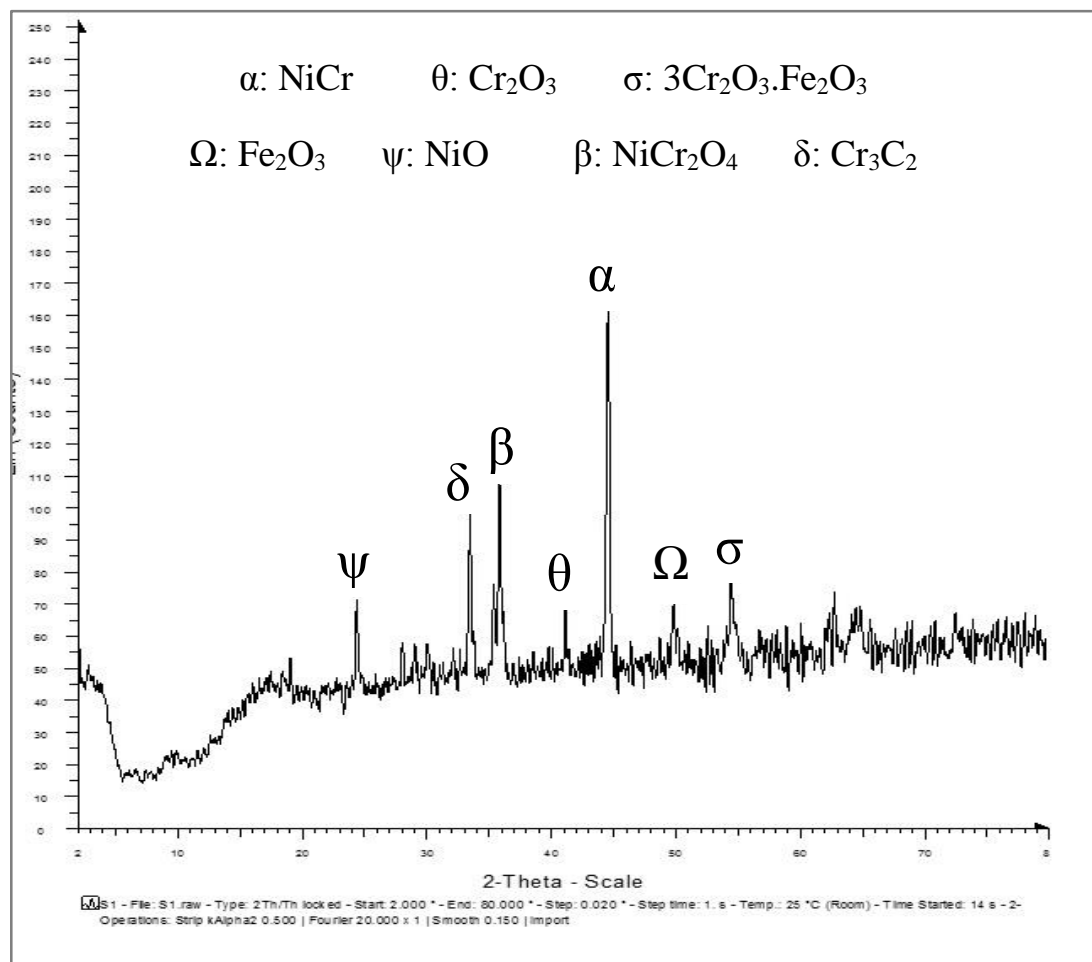


*Figure 10: X-ray diffraction patterns of bare AISI 304 stainless steel sample subjected to cyclic oxidation at  $900\text{ }^\circ\text{C}$ .*

X-ray diffraction patterns for  $\text{Cr}_3\text{C}_2$ -NiCr coated AISI 304 austenitic stainless steel sample subjected to oxidation at 900 °C, in **Figure 11** shows NiC,  $\text{Fe}_2\text{O}_3$ , and  $3\text{Cr}_2\text{O}_3.\text{Fe}_2\text{O}_3$  as major phases detected. The minor phases are  $\text{Cr}_2\text{O}_3$  and  $\text{NiCrO}_4$ .

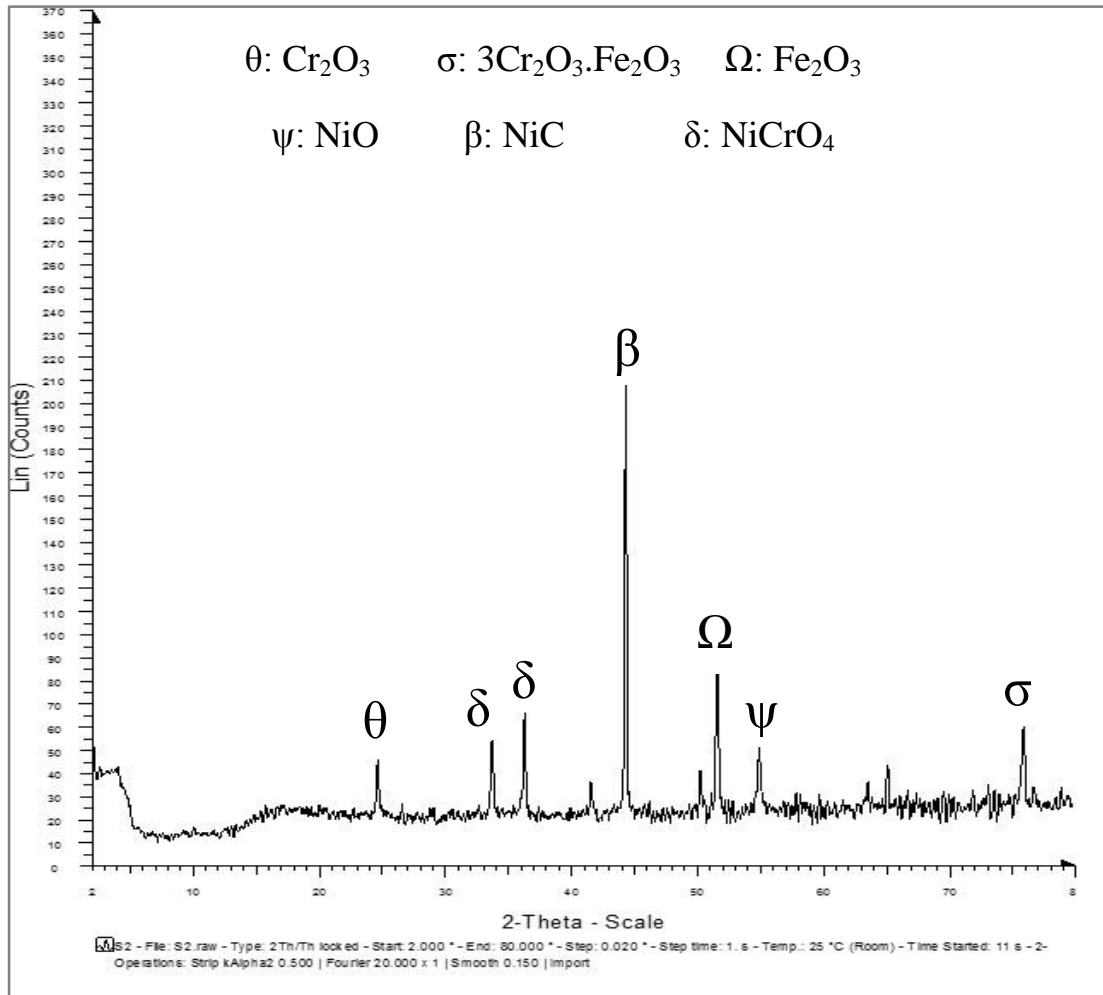


*Figure 11: X-ray diffraction patterns of  $\text{Cr}_3\text{C}_2$ -NiCr-coated AISI 304 stainless steel sample subjected to cyclic oxidation test at 900 °C*

For bare austenitic stainless steel AISI 304 sample exposed to hot corrosion in highly corrosive,  $\text{Na}_2\text{SO}_4$ , medium at 900 °C, XRD patterns detect major phases such as  $\text{Ni}_3\text{S}_4$  and  $\text{NiCr}_2\text{O}_4$ . The minor phases identified were  $\text{Cr}_2\text{S}_3$ ,  $3\text{Cr}_2\text{O}_3\cdot\text{Fe}_2\text{O}_3$ ,  $\text{Cr}_3\text{C}_2$ , and  $\text{Fe}_2\text{O}_3$  as displayed in **Figure 12**.

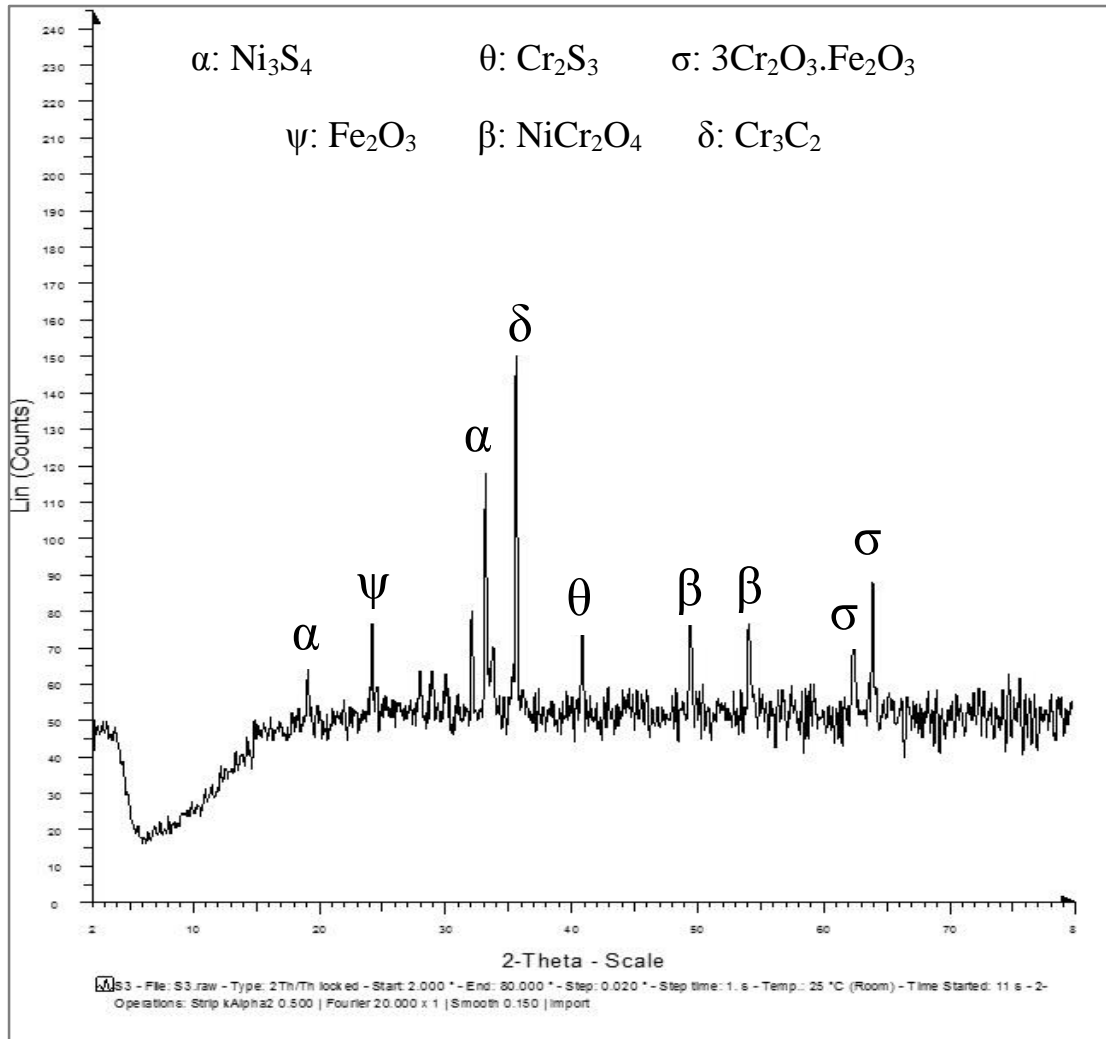


*Figure 12: X-ray diffraction patterns of bare AISI 304 stainless steel subjected to cyclic hot corrosion test at 900 °C*

X-ray diffraction patterns for  $\text{Cr}_3\text{C}_2$ -NiCr coated AISI 304 austenitic stainless steel sample exposed to hot corrosion at 900 °C, have been presented in **Figure 13**. As it indicates, the major phases identified were  $\text{NiCr}_2\text{O}_4$ , NiCr, and  $\text{NiFeO}_4$ . As for the minor phases  $\text{Cr}_2\text{O}_3$ ,  $\text{Ni}_3\text{S}_4$ ,  $\text{Cr}_3\text{C}_2$ , and  $3\text{Cr}_2\text{O}_3.\text{Fe}_2\text{O}_3$  were detected.

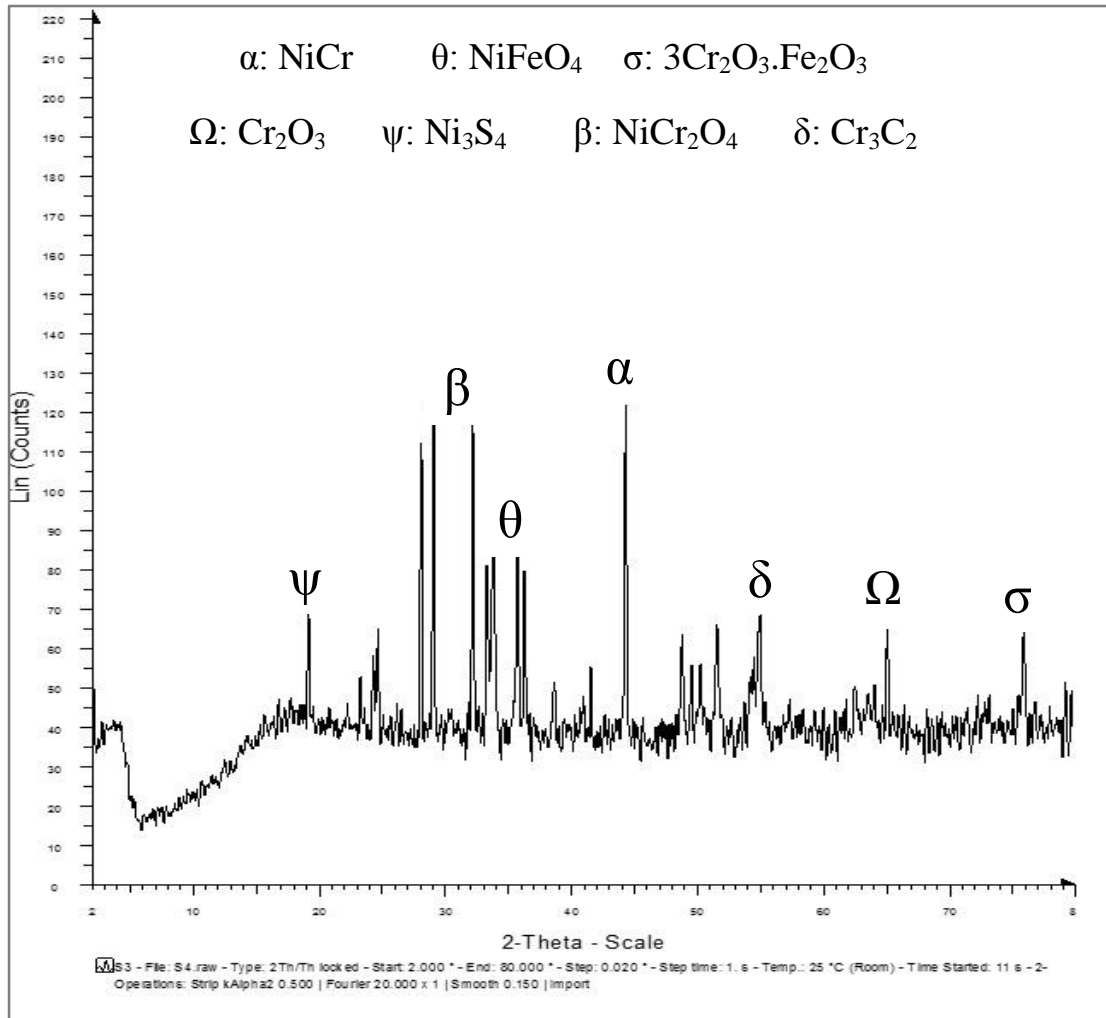


*Figure 13: X-ray diffraction patterns of  $\text{Cr}_3\text{C}_2$ -NiCr-coated AISI 304 stainless steel sample subjected to cyclic hot corrosion test at 900 °C*

### 4.3 FE-SEM/EDAX analysis

#### 4.3.1 Surface morphology of the scales

FE-SEM micrographs with EDS spectrum reveals the surface morphology of the Cr<sub>3</sub>C<sub>2</sub>-NiCr-coated and bare substrate samples after cyclic oxidation and hot corrosion tests in air and Na<sub>2</sub>SO<sub>4</sub> medium, respectively, for 20 hrs at 900 °C as shown in **Figures 14-17**.

The surface scale developed on bare AISI 304 stainless steel samples subjected to cyclic oxidation **Figures 14**, is massive, with dense clusters mainly consisting of Cr and O, in which, irregular Cr discs distributed throughout the coating. The scales revealed the presence of Cr, Fe and O rich elements, thereby suggesting the formation of Cr<sub>2</sub>O<sub>3</sub>, Fe<sub>2</sub>O<sub>3</sub> and their spinels (NiCr<sub>3</sub>O<sub>4</sub>). The presence of these phases in the top scale of coated superalloys is further supported by the XRD and X-ray mapping analysis.

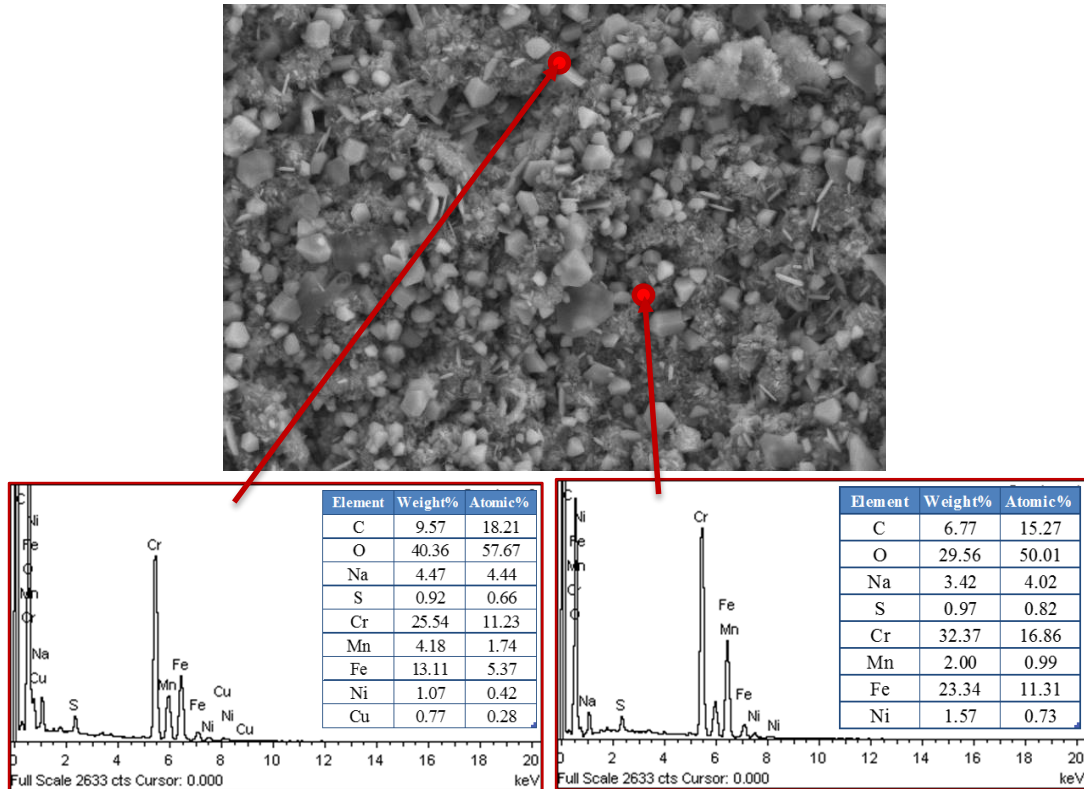


*Figure 14: FE-SEM/EDAX analysis along with EDS spectrum for bare AISI 304 subjected to cyclic oxidation in air at 900 °C.*

Similarly, the scale formed on the bare AISI 304 stainless steel samples exposed to hot corrosion depicts the presence of Cr, Fe, and O causing the formation of  $\text{Cr}_2\text{O}_3$  and  $\text{Fe}_2\text{O}_3$  as predominant oxides, **Figure 15**.

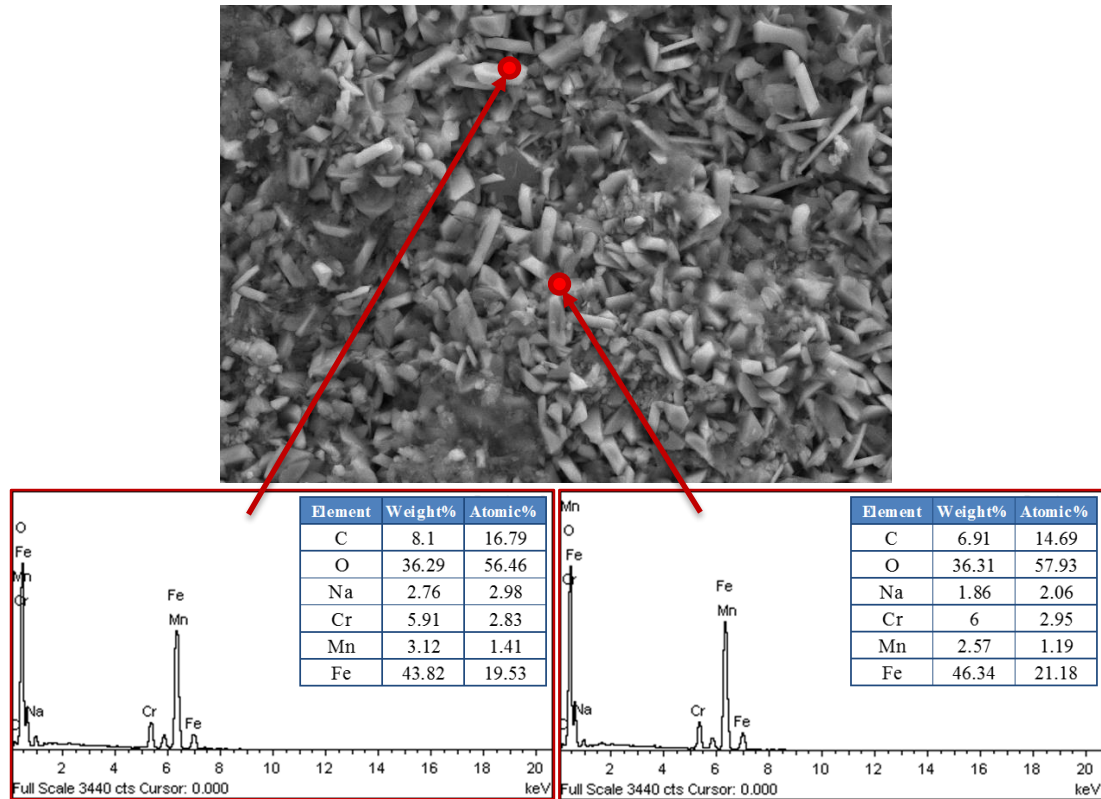


*Figure 15: FE-SEM/EDAX analysis along with EDS spectrum for bare AISI 304 subjected to cyclic hot corrosion in  $\text{Na}_2\text{SO}_4$  at  $900^\circ\text{C}$ .*

FE-SEM/EDAX analysis of phases for  $\text{Cr}_3\text{C}_2$ -25NiCr coated AISI 304 samples is shown in **Figures 16 and 17**. They show that the top surface of the coating mostly has a homogeneous, adherent and non-uniform oxide scale with variable thickness of NiO scale is formed. Cr and Ni rich splats are formed, presence of more than 25 wt% oxygen at coating-substrate interface indicates a thick band of  $\text{Cr}_2\text{O}_3$ .

The oxidised  $\text{Cr}_3\text{C}_2$ -NiCr coated AISI 304 sample has two regions, one with dark grey patches composed of Cr and the light grey patches show Ni rich splats. FE-SEM image shows the formation of a compact, adherent and continuous oxide scale. EDAX analysis of sample reveals **Figure 16**, that the uppermost part of the scale has higher concentration of Cr, while Ni-rich splats in the subscale region. It indicates the presence of continuous, adherent and non-uniform oxide scale with variable thickness of  $\text{Cr}_2\text{O}_3$ .

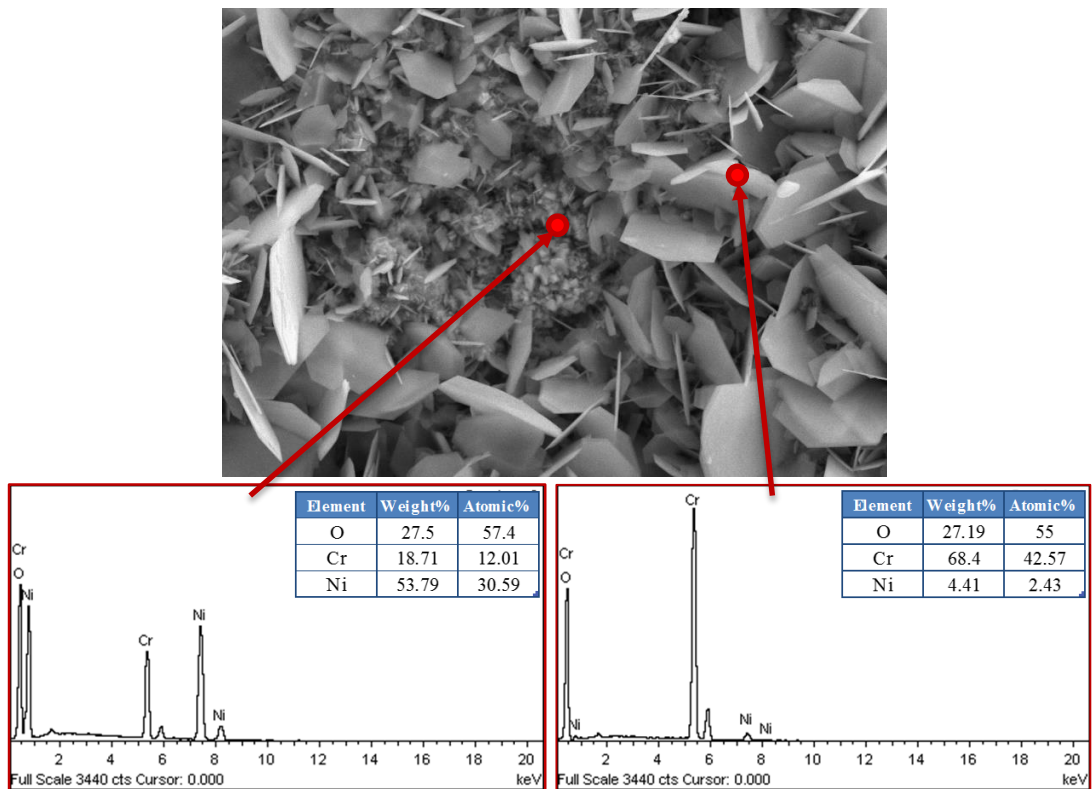


Figure 16: FE-SEM/EDAX analysis along with EDS spectrum for  $Cr_3C_2-NiCr$  coated AISI 304 subjected to cyclic oxidation in air at 900 °C

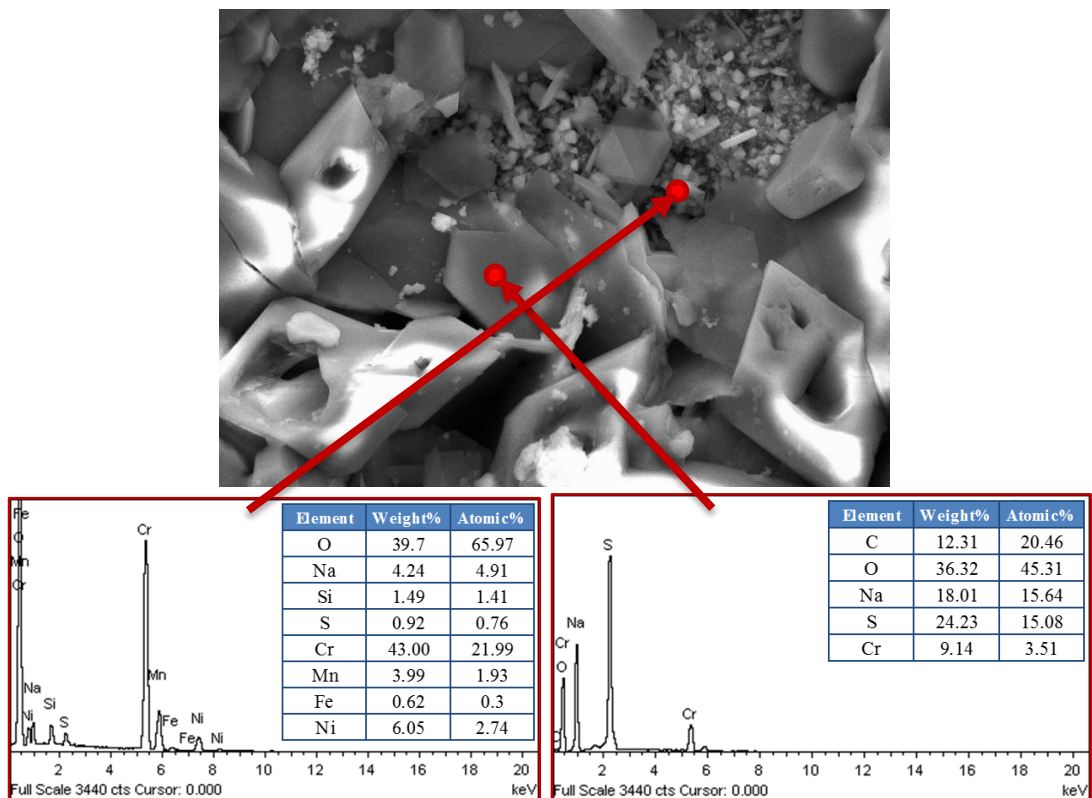
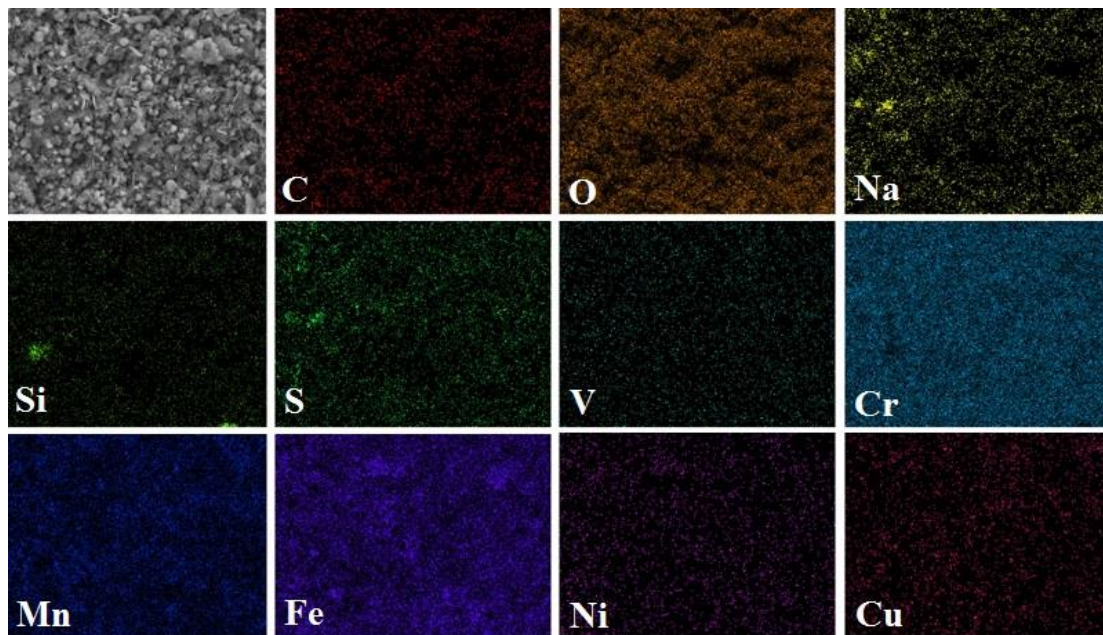


Figure 17: FE-SEM/EDAX analysis along with EDS spectrum for  $Cr_3C_2-NiCr$  coated AISI 304 subjected to cyclic hot corrosion in  $Na_2SO_4$  at 900 °C.

The EDAX analysis of hot corroded  $\text{Cr}_3\text{C}_2\text{-NiCr}$  coated scale shows the formation of  $\text{Cr}_2\text{O}_3$  and  $\text{NiO}$  as major phases on the AISI 304 sample as shown in **Figure 17**. The presence of these elements indicates that these elements may have diffused from the substrate to the uppermost part of the scale during hot corrosion of the specimen at  $900\text{ }^\circ\text{C}$ .

#### 4.3.2 X-ray mapping

X-ray mapping of AISI 304 both bare and  $\text{Cr}_3\text{C}_2\text{-NiCr}$  coated samples, that were subjected to cyclic oxidation at  $900\text{ }^\circ\text{C}$  for 20 hours, **Figures 18 and 19**, shows very thin oxide scale mainly consisting of chromium in the top scale, in the sub scale region, Ni-rich splats are found mostly at places where Cr is depleted. Oxygen penetration is restricted to the top surface of the coating but its presence at the coating–substrate interface may be either due to the in-flight oxidation of coating material or oxygen might have penetrated during initial cycles of air oxidation run along the inter-splat boundaries.



*Figure 18: Composition image (SEI) and X-ray mapping of bare AISI 304 subjected to cyclic oxidation in air at  $900\text{ }^\circ\text{C}$*

**Figure 19**, indicates that the coating has partially oxidised as evident from the oxygen distribution. Chromium is uniformly distributed in entire coating along the Ni-rich splat boundaries, silicon has penetrated along the coating–substrate interface, whereas iron has restricted up to the coating–substrate interface.

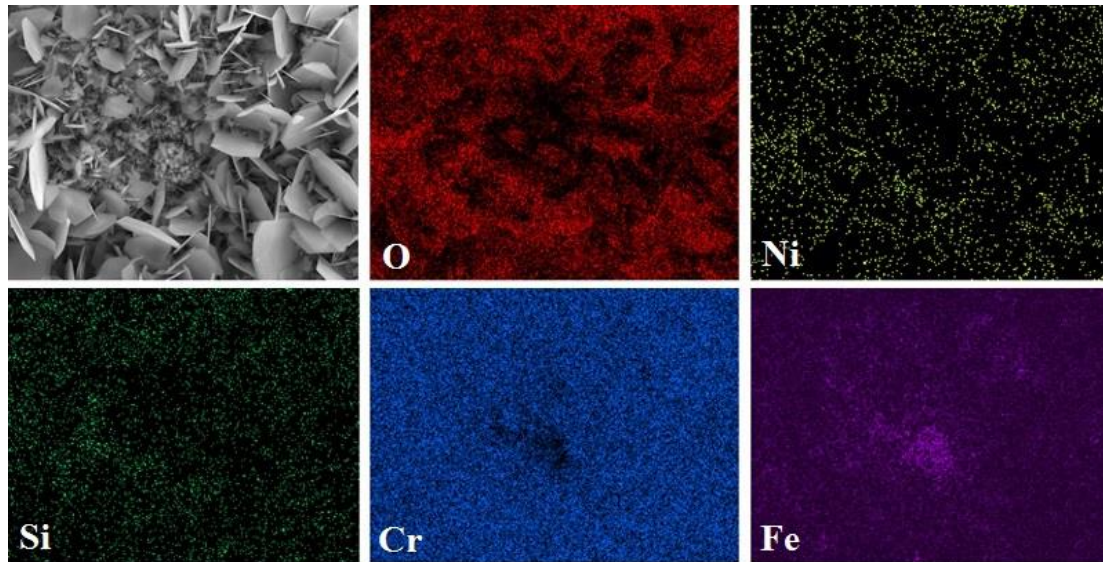


*Figure 19: Composition image (SEI) and X-ray mapping of  $\text{Cr}_3\text{C}_2\text{-NiCr}$  coated AISI 304 subjected to cyclic oxidation in air at 900 °C*

X-ray mapping of AISI 304 both bare and  $\text{Cr}_3\text{C}_2\text{-NiCr}$  coated samples, which were exposed to cyclic hot corrosion at 900 °C for 20 hours in molten salt environment ( $\text{Na}_2\text{SO}_4$ ), were analysed for different elements across the scale using Composition image (SEI) and X-ray mapping analysis **Figure 20 and 21**.

The X-ray mappings for hot corroded samples, indicate a variation in the thickness of the scale that mainly consists of chromium and nickel at the top surface and the rest of the coating is partially oxidised as evident from the oxygen distribution. Magnesium was found along the coating–substrate interface, also a small amount of Mn has diffused into the top surface of the coating during initial cycles of hot corrosion run, another possibility of magnesium at the coating–substrate interface may be due to entrapped particles prior to deposition of the coatings.

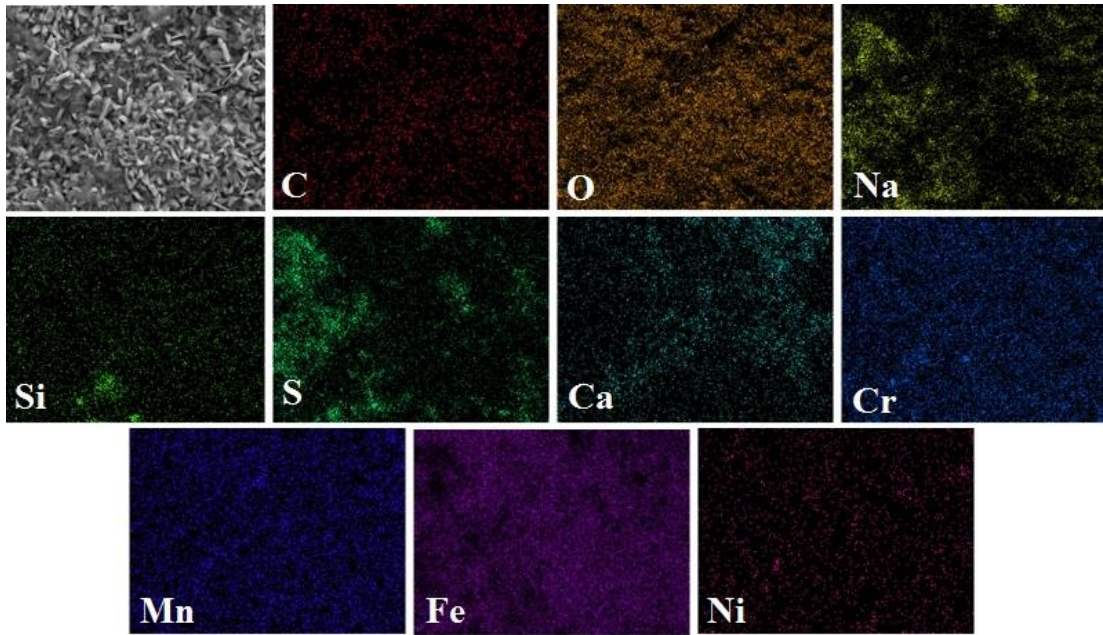


Figure 20: Composition image (SEI) and X-ray mapping of bare AISI 304 subjected to cyclic hot corrosion in  $\text{Na}_2\text{SO}_4$  at  $900^\circ\text{C}$ .

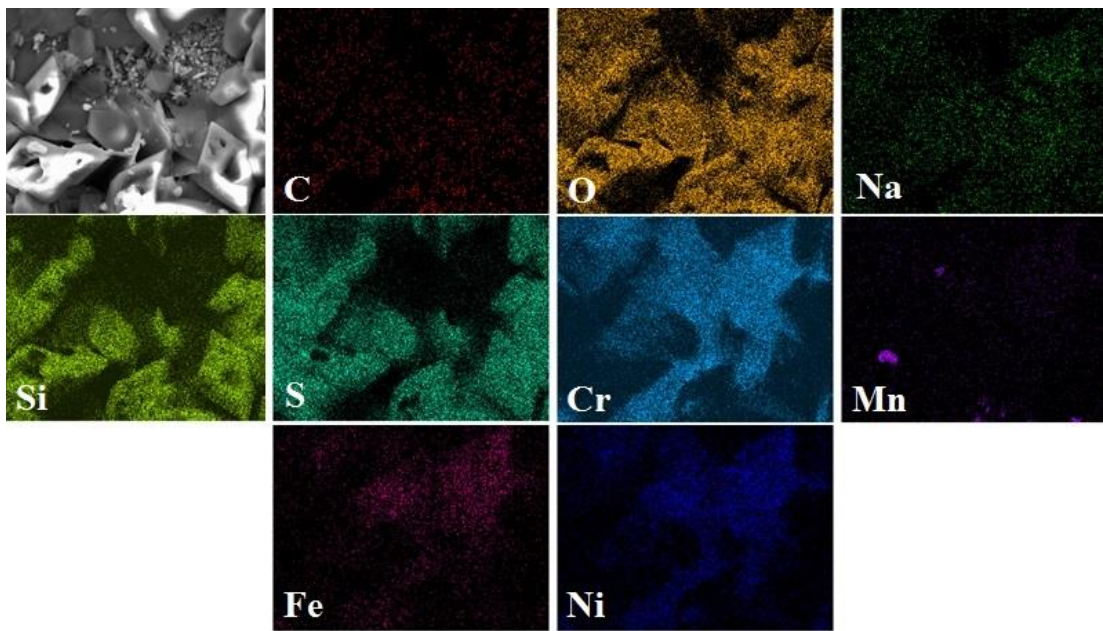


Figure 21: Composition image (SEI) and X-ray mapping of  $\text{Cr}_3\text{C}_2$ -NiCr coated AISI 304 subjected to cyclic hot corrosion in  $\text{Na}_2\text{SO}_4$  at  $900^\circ\text{C}$ .

### 4.3 Discussion

The weight change data for austenitic stainless steel AISI 304 exposed to hot corrosion and oxidation tests in air and Na<sub>2</sub>SO<sub>4</sub> environment, are plotted in **Figures 8a and 8b**. The tests were carried out on both bare and Cr<sub>3</sub>C<sub>2</sub>-NiCr coated samples. Also test were conducted in intervals for 20 hours, every 3 hours the specimens were taken out of the furnace and cooled at room temperature (25 °C), this is done to simulate actual operating conditions for tested material.

The graph shows that all oxidized samples undergo a lesser weight change, compared to the hot corroded samples. This occurrence might be due to the oxides rapidly formed at the boundaries and within pores, similarly because of this oxide layers the following weight change was steady. During these cycles, specimens subjected to hot corrosion started spalling/sputtering, making difficult to take weight change measurements precisely and accurately. The cumulative weight gain after 20 hours of oxidation and hot corrosion at 900°C is shown in **Figures 9a and 9b**.

Poor corrosion resistance of bare austenitic stainless steel, is due to intense spallation and sputtering, which can be attributed to the severe strain developed as a result of Fe<sub>2</sub>O<sub>3</sub> precipitation from the liquid phase and the inter-diffusion of intermediate layer of iron oxide. It is inferred that the steel substrates are more prone to hot corrosion in molten salt environment.

The initial higher oxidation rate of the coated specimens might be attributed due to air which is entrapped during HVOF deposition and sheltered in the pores, since the cooling of the coating was rapid; there is shortage of time for the residual air to react with the surrounding coating alloys. However, the coating underwent in-situ reaction during high temperature oxidation (900 °C) and was partially oxidised, during the subsequent cycles, the formation of oxides has blocked the pores and acted as diffusion barriers to the inward diffusion of corrosive species. This leads to a slow oxide scale growth; consequently the weight gain is low. Chromium exhibits higher affinity for oxygen to form Cr<sub>2</sub>O<sub>3</sub> during the earlier stages of hot corrosion. This shows that the oxidation resistance of Cr<sub>3</sub>C<sub>2</sub>-NiCr coating is solely based on the formation of Cr<sub>2</sub>O<sub>3</sub>, which acts as a diffusion barrier for the corrosive species.

Once the oxides are formed at the places of porosity, the growth of the oxides becomes limited mainly to the surface of the specimens. This would relatively minimize the weight gain and result in the steady state oxidation behaviour with the progress of long term high temperature exposure, which are in accordance with the similar observation reported by Choi (2012) and Niranatlumpong (2013). Poor corrosion resistance of uncoated samples is due to intense spallation and sputtering which can be attributed to the severe strain developed as a result of  $\text{Fe}_2\text{O}_3$  precipitation from the liquid phase and the inter diffusion of intermediate layer of iron oxide. Presence of Si, Al, Fe, Mn and K phases in a thin layer might have imposed severe strain on the scale, which may result in the spallation, cracking and exfoliation of the oxide scale, the cracks might have allowed the corrosive liquid to reach the metal substrate. The presence of  $\text{Fe}_2\text{O}_3$  in the spalled scale has also been reported to be non-protective by Shimizu (2013) during their hot corrosion study on HVOF-sprayed  $\text{Cr}_3\text{C}_2$ -NiCr-coating on Fe- and Ni-based superalloys in a  $\text{Na}_2\text{SO}_4$ -60%  $\text{V}_2\text{O}_5$  at 900 °C under cyclic conditions for 50 cycles.

XRD analysis of hot corroded superalloy indicates the formation of NiO,  $\text{Cr}_2\text{O}_3$  and spinel as major phases. The predominant phases formed on oxidized samples are  $\text{NiCr}_2\text{O}_4$ ,  $\text{Cr}_2\text{O}_3$  and  $\text{Fe}_2\text{O}_3$ , whereas hot corroded shows  $\text{Fe}_2\text{O}_3$ ,  $\text{Ni}_3\text{S}_4$  and  $\text{Cr}_2\text{O}_3$  as major phases, **Figures 10-13**.

In all the samples Na, Cr and O show their presence in entire scale mainly at splat boundaries showing their penetrating nature into the scale through the splat boundaries. O penetration is restricted mainly to the upper most part of the scale. Si and Fe elements of the substrate, in general, show their diffusion behaviour from the substrate to the top scale. SE X-ray mapping of hot corroded and oxidized  $\text{Cr}_3\text{C}_2$ -NiCr coated AISI 304 specimens, show that the oxide scale exhibits dense structure and mainly consists of Cr in which Ni rich splats are present, **Figures 19 and 21**. On the other hand, X-ray mappings for bare AISI 304 samples subjected to oxidation and hot corrosion in an environment of air and  $\text{Na}_2\text{SO}_4$ , respectively, at 900 °C for 20 hours **Figures 18 and 20**, indicate the formation of relatively dense scale of  $\text{Cr}_2\text{O}_3$ , NiO and  $\text{NiCr}_2\text{O}_4$ . The upper most part of the scale is primarily shows some traces of Si and Fe, which might have diffused from substrate to the scale; Si is also present along the splat boundaries of coating substrate interface.

## CHAPTER 5

### CONCLUSION AND RECOMMENDATION

#### 5.1 Conclusion

Oxidation and hot corrosion behaviour study of Cr<sub>3</sub>C<sub>2</sub> 25 (Ni20Cr) thermal spray coating is very essential in nowadays industry. Growing demand on production, leads to development of highly durable materials. The use Austenitic Stainless Steel (AISI 304) by quality of their excellent high temperature properties coupled with oxidation/corrosion resistance, have been widely used in industry and many more applications are still to be researched, where these materials may have prominent potential. Hence, several coating techniques have been developing, which are proven to be convenient, safe and economically feasible.

HVOF spraying process has been successfully used to deposit Cr<sub>3</sub>C<sub>2</sub>-NiCr coating on austenitic stainless steel substrates in the range of 200–250 μm thickness, the coating has nearly uniform, adherent and dense microstructure with porosity less than 0.8%.

Based on the findings, Cr<sub>3</sub>C<sub>2</sub>-NiCr coating on AISI 304 substrates has been uniformly deposited by HVOF spraying process in the present work and the following conclusions are made:

- ❖ The HVOF Cr<sub>3</sub>C<sub>2</sub>-NiCr coatings on austenitic stainless steel specimens when subjected to cyclic oxidation/hot corrosion test in air and Na<sub>2</sub>SO<sub>4</sub> solution at 900 °C for 20 hours were found to be successful in maintaining its adherence with the substrate metals. The oxide scales were also found to be intact and with some indication of spalling in hot corroded bare sample.

- ❖ Initial spallation and sputtering might be due to the different values of thermal expansion coefficients of the coatings, substrate and oxides. Some elements of the substrate such as Fe, Cr, Si, and Mn showed a tendency of outward diffusion from the substrate.
- ❖ The weight gain data for all the Cr<sub>3</sub>C<sub>2</sub>-NiCr-coated samples showed a less weight change compared to bare samples. Also oxidised samples indicated lesser weight change in contrast of hot corroded samples.
- ❖ The Cr<sub>3</sub>C<sub>2</sub>-NiCr coating after exposure to air oxidation and hot corrosion showed the presence of mainly oxides of Cr and Ni in the upper region of the scale. In the subscale region, the phases revealed were oxides of Cr and Fe, and their spinels
- ❖ The oxides of chromium and nickel, and their spinels may be contributing to blocking the transport of degrading corrosive species through the Cr<sub>3</sub>C<sub>2</sub>-NiCr coating and thus contributed to hot corrosion resistance.
- ❖ The hot corrosion resistance of the coating is also partly attributable to the presence of very low porosity, uniform fine grains and the flat splat microstructure of Cr<sub>3</sub>C<sub>2</sub>-NiCr coating obtained by HVOF process.

## 5.2 Recommendation

Although the Austenitic Stainless Steel (AISI 304) is commonly used material, author would recommend, further studies should be done by trying existing coating techniques, but using different powders and different substrate materials that never been used for, to study the probability of increasing the effectiveness of the coatings. Also author would recommend studying on different behaviours such as erosion, wear characteristics of various substrates coated with different powders, and techniques.

## REFERENCES

- Amardeep Singh Kang, Jasmaninder Singh Grewal, Deepak Jain, Shivani Kang. (2012). Wear Behavior of Thermal Spray Coatings on Rotavator Blades. *Journal of Thermal Spray Technology*, 21(2), 355-359.
- Cho, T. Y., Yoon, J. H., Cho, J. Y., Joo, Y. K., Kang, J. H., Zhang, S., Kwon, S. C. (2009). Surface Properties and Tensile Bond Strength of HVOF Thermal Spray Coatings of WC-Co Powder onto the Surface of 420J2 Steel and the Bond Coats of Ni, NiCr, and Ni/NiCr. *Surface & Coatings Technology*(203), 3250-3253.
- D. K. Goyal, H. Singh, H. Kumar. (2011). An overview of slurry erosion control by the application of high velocity oxy fuel sprayed coatings. *Journal of Engineering Tribology* 225(11), 1092-1105.
- Davis, J. R. (2004). *Thermal Spray Technology*. Ohio: ASM International.
- Deepti Rawat, Pradeep Barthwal, Amit Joshi. (2013). *Carbide coatings on hot working steel (Cr high alloy H-13 steel) by Detonation Gun Process*. Paper presented at the IRAJ International Conference, Delhi.
- Hermanek, F. J. (2014). Thermal Spraying: What it Was and What it Has Become. from <http://www.thermalspray.org/images/thermal-spray-coatings2.jpg>
- Jianqiang Zhang, Xiao Peng, David J. Young, Fuhui Wang. (2013). Nano-crystalline coating to improve cyclic oxidation resistance of 304 stainless steel. *Surface & Coatings Technology*(217), 162-171.
- M. Mamatha Kumari, S. Natarajan, J. Alphonsa, S. Mukherjee. (2010). Dry sliding wear behaviour of plasma nitrocarburised AISI 304 stainless steel using response surface methodology. *Surface Engineering*, 26(3), 191-198.
- N. Jegadeeswaran, M. R. Ramesh, K. Udaya Bhat. (2014). Oxidation Resistance HVOF Sprayed Coating 25% (Cr<sub>3</sub>C<sub>2</sub>-25(Ni<sub>20</sub>Cr)) + 75%NiCrAlY on Titanium Alloy. *Procedia Materials Science*(5), 11-20.

- N. Padhy, Subhash Kamal, Ramesh Chandra, U. Kamachi Mudali, Baldev Raj. (2010). "Corrosion performance of TiO<sub>2</sub> coated type 304L stainless steel in nitric acid medium". *Surface and Coating Technology*(204), 2782-2788.
- Subhash Kamal, R. Jayaganthan, S. Prakash, Sanjay Kumar. (2008). Hot corrosion behavior of detonation gun sprayed Cr<sub>3</sub>C<sub>2</sub>-NiCr coatings on Ni and Fe-based superalloys in Na<sub>2</sub>SO<sub>4</sub>-60% V<sub>2</sub>O<sub>5</sub> environment at 900 °C. *Journal of Alloys and Compound*(463), 359-372.
- Subhash Kamal, R. Jayaganthan, Satya Prakash. (2009). Evaluation of cyclic hot corrosion behaviour of detonation gun sprayed Cr<sub>3</sub>C<sub>2</sub>-25%NiCr coatings on nickel- and iron-based superalloys. *Surface & Coatings Technology*, 203, 1004-1013.
- Y.F. Yan, X.Q. Xu, D.Q. Zhou, H. Wang, Y.Wua, X.J. Liu, Z.P. Lu. (2013). Hot corrosion behaviour and its mechanism of a new alumina-forming austenitic stainless steel in molten sodium sulphate. *Corrosion Science*, 77, 202-209.
- Rogne, T. & Berget, T. (2004). Investigations of corrosion properties of different ceramic-metallic coatings sprayed the HVOF process. *Proceedings of the International Thermal Spray Conference*, 433 – 438.
- Shimizu, Y., Sakaki, K., Yoshikane, T., Fujioka, J., & Komatz, M. (2004). HVOF sprayed Cr<sub>3</sub>C<sub>2</sub>-NiCr Cermet Coating to Improve the Erosion Resisting Performance of the Coal Burning Boiler Tube. *Thermal Spray*. Osaka.
- Uozato, S., Nakata, K., & Ushio, M. (2003). Corrosion and wear behaviours of ferrous powder thermal spray coatings on aluminium alloy. *Surface and Coatings Technology* (169 – 170), 691 – 694
- Berget, J., & Rogne, T. (2004). Erosion and Erosion-Corrosion Properties of HVOF Sprayed Tungsten Carbide (WC) Coatings with High Alloy Binders. *Thermal Spray*. Osaka.

## APPENDIX

### SULZER METCO DIAMALLOY 3004 MATERIAL SAFETY DATA SHEET

Diamalloy 3004 is a blend (75/25) of very fine particles of chromium carbide and nickel chromium powders. When properly sprayed using the Diamond Jet process, it produces coatings which are very hard, dense and well bonded. Diamalloy 3004 is harder than standard chromium carbide coatings and is second in hardness only to Diamalloy 3007. Because of its unique combination of properties, Diamalloy 3004 is recommended for resistance to wear by fretting, abrasive particles and hard surfaces in the temperature range 540 – 815 °C (1000 – 1500 °F).

#### Typical applications:

- ❖ Turbine Air Seal Rings
- ❖ Turbine Baffle Dampers
- ❖ Turbine Inner Nozzle Supports
- ❖ Fuel Rod Mandrels
- ❖ Hot Crushing Rolls

#### Gun spray parameters

Injector:	#3	Shell:	A
Insert:	#3	Siphon Plug:	#2
Air Cap:	#2		

Gases	Oxygen	Propylene	Air
Pressure, psi (bar)	150 (10.3)	100 (6.9)	75 (5.2)
Flow (FMR)	42	38	47
SCFH (SLPM)	606 (265.4)	168 (73.6)	742 (325.0)
BTU/hr × 10 <sup>3</sup> (joules/hr × 10 <sup>6</sup> )	-	367 (3.87)	-



*Figure A.1: Vacuum blast machine with working sandblast pressure of 40 psi*

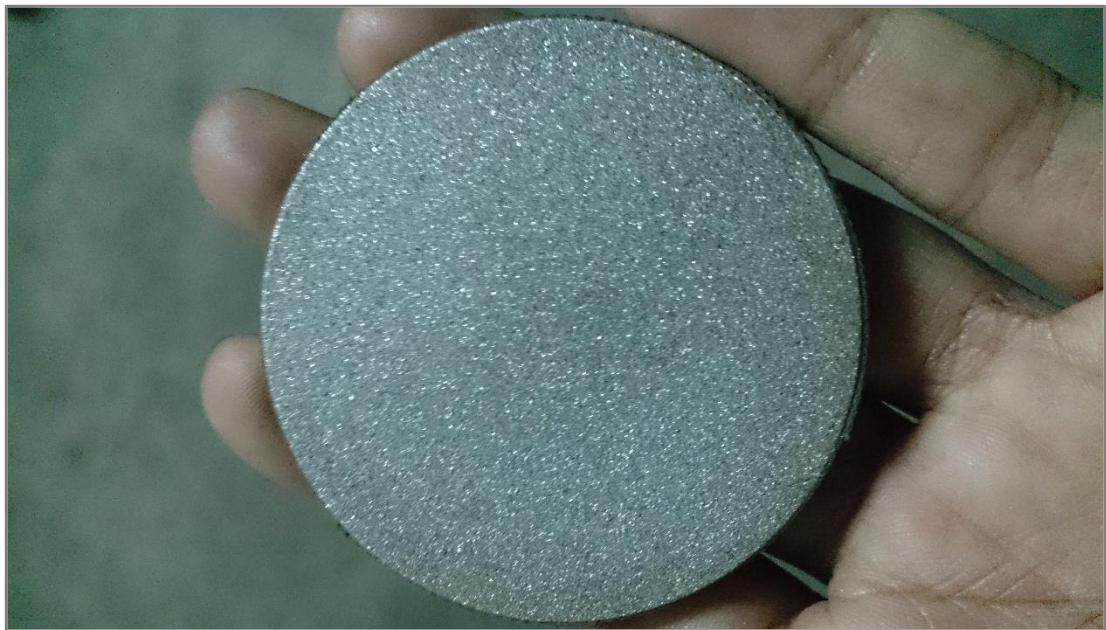


*Figure A.2: Substrate surface after sandblasting process*



*Figure A.3: HVOF gun connected to the powder feeder and fuel/air flow*

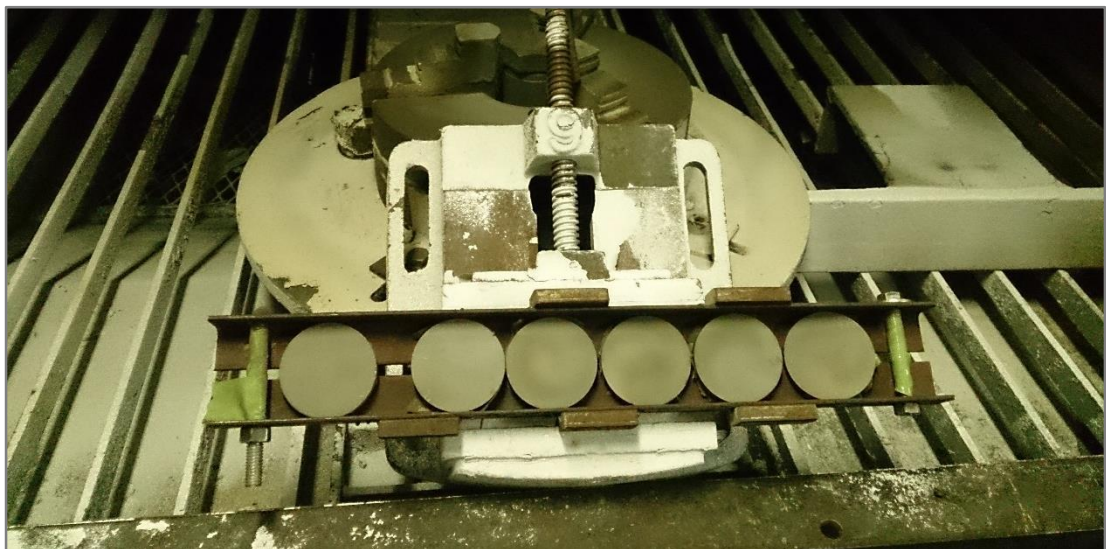


*Figure A.4: Samples clamped in place for HVOF coating procedure*



*Figure A.5: HVOF coating procedure*

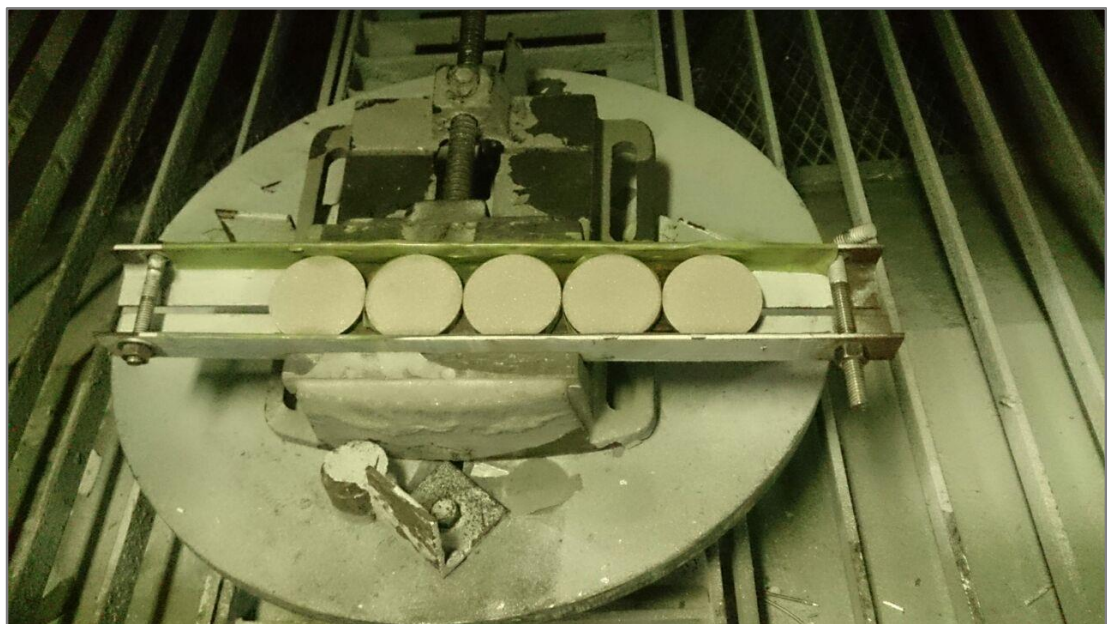


*Figure A.6: Samples after coating procedure*

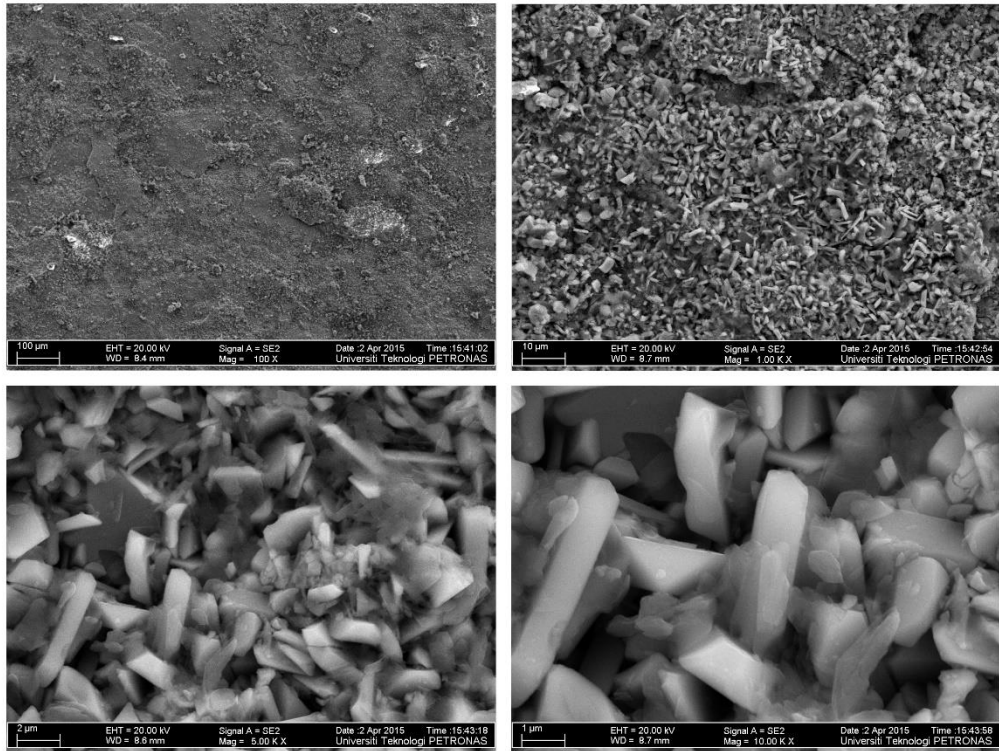


*Figure A.7: Surface images of AISI 304 stainless steel sample subjected to cyclic hot corrosion test at 900 °C*

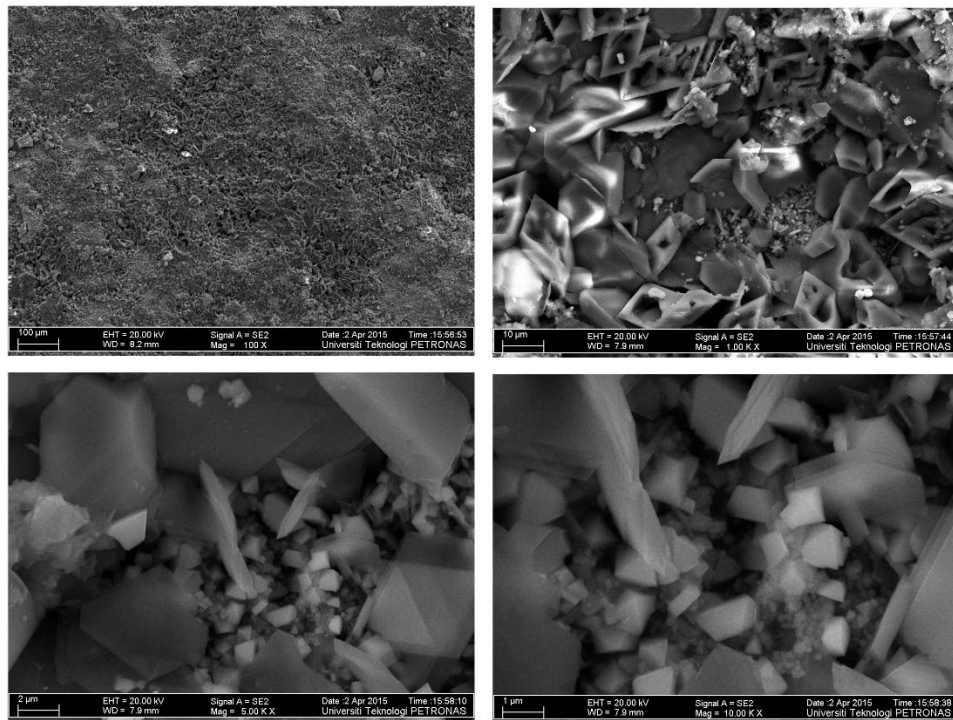


*Figure A.8: Surface images of Cr<sub>3</sub>C<sub>2</sub>–NiCr-coated AISI 304 stainless steel sample subjected to cyclic hot corrosion test at 900 °C*

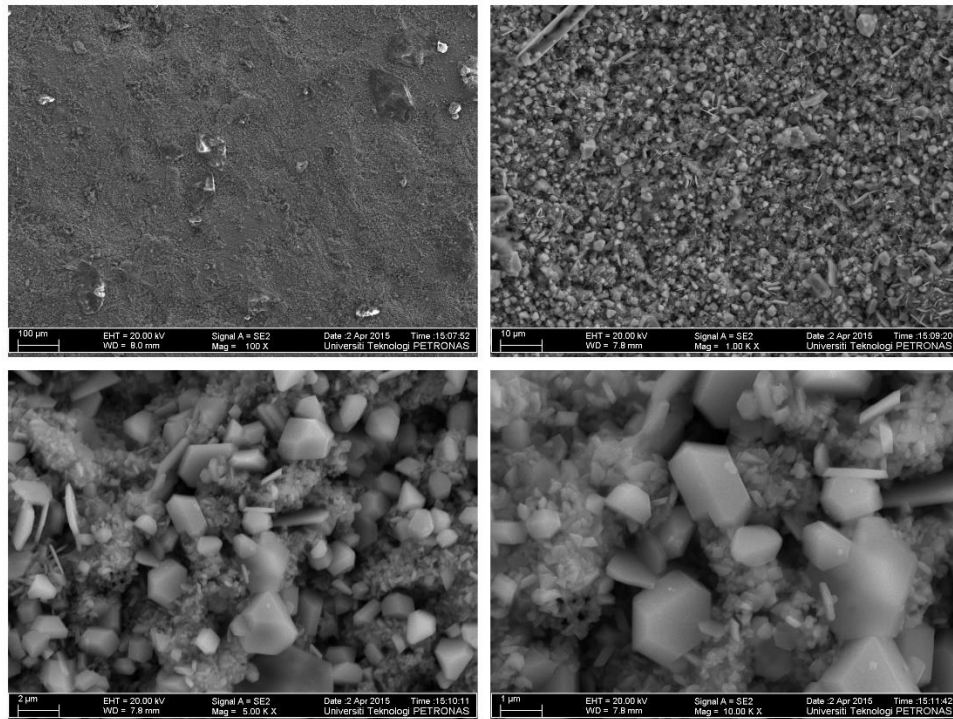


Figure A.9: Surface images of AISI 304 stainless steel sample subjected to cyclic oxidation test at 900 °C

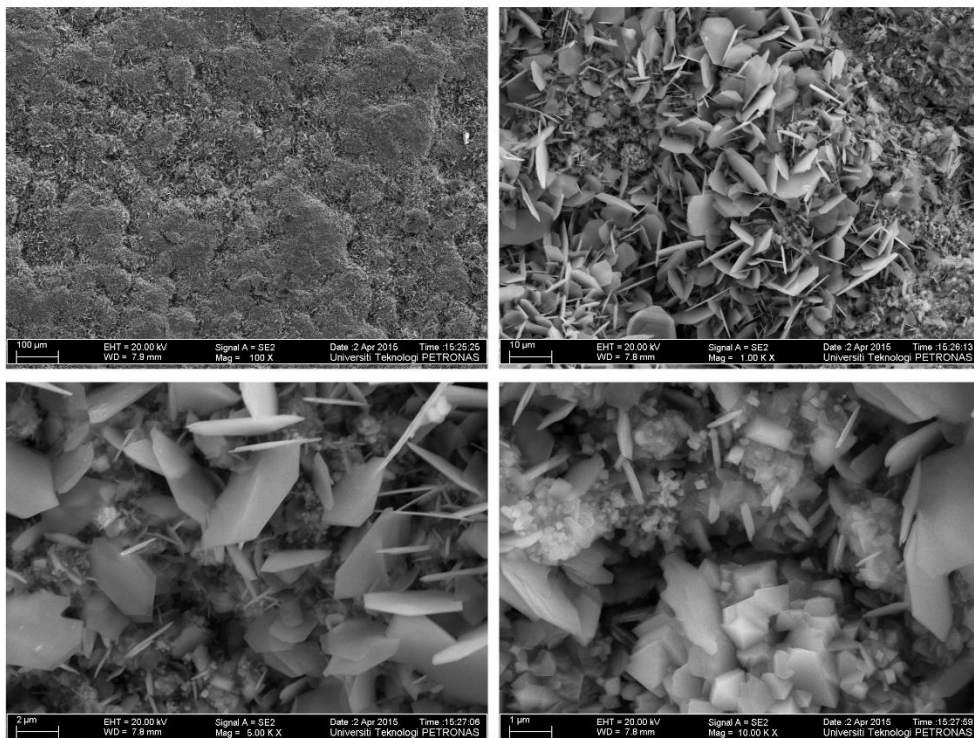


Figure A.10: Surface images of Cr<sub>3</sub>C<sub>2</sub>-NiCr-coated AISI 304 stainless steel sample subjected to cyclic oxidation at 900 °C